Static analysis of functionally graded plates using new nonpolynomial displacement fields via Carrera Unified Formulation

Static analysis of functionally graded plates using new non-polynomial displacement fields via Carrera Unified Formulation

J.L. Mantari [a], I.A. Ramos [b], E. Carrera[c], M . Petrolo[c]

[a] Faculty of Mechanical Engineering, Universidad de Ingeniería y Tecnología (UTEC), Santa Anita, Lima, Peru

[b] Faculty of Mechanical Engineering, Universidad Nacional de Ingeniería, Av. Túpac Amaru 210, Rimac, Peru

[c] Department of Mechanical and Aerospace Engineering, Politecnico di Torino, Corso Duca degli Abruzzi 24, Torino, Italy

Revised form of Ms. Ref. No.: JCOMBD1501422

Author for correspondence:

E. Carrera, Professor of Aerospace Structures and Aeroelasticity,

Department of Mechanical and Aerospace Engineering,

Politecnico di Torino,

Corso Duca degli Abruzzi 24,

10129 Torino, Italy,

tel: +39 011 090 6836,

fax: +39 011 090 6899,

e-mail: erasmo.carrera@polito.it

Abstract

This paper presents a static analysis of functionally graded (FG) single and sandwich plates using Carrera's Unified Formulation with five new displacement fields of the non-polynomial form. In particular, trigonometric, exponential and hyperbolic displacement fields are employed. The simply supported FG single and sandwich plates are subjected to a bi-sinusoidal load. The governing equations for the static bending analysis are obtained employing the Principal of Virtual Displacement (PVD) under CUF and solved using Navier type solutions. The results show that non-polynomial thickness functions are accurate although, in a few cases, the influence of some non-polynomial terms may be detrimental.

Keywords: Static analysis, functionally graded materials, Carrera Unified Formulation, non-polynomials functions.

1. Introduction

Functionally graded materials (FGMs) are composite materials formed of two or more constituent phases with a continuously variable distribution by gradually changing the volume fraction. The conventional laminated materials suffer from discontinuity of materials properties in the bonded of the layers. As a result, stress concentration occurs at the interface. FGMs born to eliminate these problems due to bonding of two discrete materials. FGMs have been proposed, developed and successfully used in industrial application since 1980s [1]. These materials were designed as a thermal barrier coating in aerospace application, such as ceramic-metal composite structure. Nowadays, FGMs are alternative materials widely used in aerospace, civil, mechanical, nuclear, optical, electronic, chemical, shipbuilding, and biomechanical industries.

There are various theories for the modeling and different methods to study FGMs. Thai and Kim [2] and Swaminathan et al. [3] have presented comprehensive review papers of several theories for modeling and analysis of FG plates for the stress, vibration and buckling analysis.

In this context, the classical plate theory model (CPL) or Kirchoff theory, which ignores the normal and shear deformation effect, only give acceptable results for thin plates. Then the first order shear deformation (FSDT) based in Reissner and Mindlin was utilized but this theory needs a shear correction factor, which is difficult to calculate. Therefore higher-order shear deformation theories (HSDTs) were introduced to avoid the shear correction factors. The HSDTs can be classified in different models, such as equivalent single layer (ESL), quasi-layer-wise and layer-wise models in [4-8]. Further, The HSDTs can be developed using polynomial [9-10] or non-polynomial thickness functions [11-20]. The majority of these theories do not account for transverse extensibility by neglecting the transverse normal stresses, σ_{zz}. The effects of thickness stretching in FG plates and shells were developed by Carrera et al. [21].

The Carrera's Unified Formulation (CUF) was formulated by Carrera for laminated plates and shells [22-24]. CUF is a procedure to implement several plate and shell theories by expanding the displacement variables in the thickness coordinate using polynomial expansions of N-order. The CUF was developed for FGM [25-27] based on the PVD theory or the RMVT. A sinusoidal shear deformation theory (SSDT) in the CUF framework was developed by Ferreira et al. [28] for static and free vibration analysis of laminated shells. The SSDT accounts for through-the-thickness deformation, by considering a sinusoidal variation of all displacements. Neves et al.

[29-30] used a similar theory as in Ref. [28] to study the bending and free vibration of FG plates. Their formulations are based on hybrid quasi-3D sinusoidal shear deformation theory with a quadratic variation across the thickness. A quasi-3D hyperbolic shear deformation theory for the static and free vibration analysis of functionally graded plates, similar to the previous theory [29-30], was developed by Neves et al. [31-32].

This paper proposes five different and non-existent C_z^0 theories under CUF for static bending analysis of FG plates. As in Ferreira et al. [28] and Neves et al. [29-32], this work proposes trigonometric functions. Further, exponential and tangential functions are developed in this paper and compared with the polynomial thickness functions of Carrera et al. [21] for N=4. The simply supported FG plate and sandwich are subjected to a bi-sinusoidal load. The mechanical properties of the FG plates vary across the thickness direction according to a power law distribution in terms of volume fraction. The governing equations for the static analysis are obtained through Principal of Virtual Displacement (PVD) and solved using Navier type solutions.

The paper is organized as following. Section 2 outlines the mathematical modeling under CUF platform. Theoretical formulation of FGMs, displacement field, kinematic, constitutive relations, the principle of virtual works, and the governing equations are presented. Section 3 describes the solution methodology. Section 4 is about results and discussions. Finally, further general aspects are given in conclusions.

2. Analytical modeling

In a functionally graded plate (FGP) the mechanical properties can be smoothly graded from different directions and considering different shapes. This paper considers the well-known across the thickness gradation modeling of mechanical properties of FGPs. Single plates made of FGM are referred to as *plate A*. Sandwich plates made of an isotropic material (fully metal) in the bottom skin, an isotropic material (fully ceramic) in the top skin, and an FGM in the core are referred to as *plate B.*

2.1 Functionally graded plates (FGPs)

A single rectangular plate (type A) and sandwich plate (type B) of uniform thickness “h”, length “a”, and width “b” are shown in Fig. 1 and Fig. 2, respectively. The rectangular Cartesian coordinate system x, y, z, has the plane xy at z = 0, coinciding

with the mid-surface of the plate. The material properties can vary through the thickness with a power law distribution, which is defined:

$$P(z) = (P_t - P_b)V_c(z) + P_b \tag{1a}$$

$$V_c(z) = \left(\frac{z}{h} + \frac{1}{2}\right)^p, \qquad -\frac{h}{2} \le z \le \frac{h}{2} \tag{1b}$$

$$\begin{cases} V_C(\mathrm{z}) = 0 & -h/2 \le z \le h_1 \\ V_C(\mathrm{z}) = \left(\dfrac{z_c - h_1}{h_{core}}\right)^p & h_1 \le z \le h_2 \\ V_C(\mathrm{z}) = 1 & h_2 \le z \le h/2 \end{cases} \tag{1c}$$

Where P denotes the effective material property. P_t and P_b denote the property of the top and bottom faces of the plate, respectively. "p" is the exponent that specifies the material variation profile through the thickness. The effective material properties of the plate, including Young's modulus, E, and shear modulus, G, vary according to Equation (1a). $V_c(z)$ for type A and type B plates vary according to Equation (1b) and (1c), respectively (see Fig. 3 and Fig. 4). The Poisson ratio, "ν", is assumed to be constant.

2.2. Displacement base field

The CUF platform [21] states that displacement field for plates, $\boldsymbol{u}_{(x,y,z)}$, is modeled in the following manner:

$$\boldsymbol{u}(x,y,z) = F_s(z)\boldsymbol{u}_s(x,y), \quad s = 1, \dots, N$$
$$\delta\boldsymbol{u}(x,y,z) = F_\tau(z)\delta\boldsymbol{u}_\tau(x,y), \quad \tau = 1, \dots, N$$
$$F_s(z) = f_s(z), \quad F_\tau(z) = f_\tau(z), \tag{2a-c}$$

where F_s and F_τ are function of z. $\boldsymbol{u}_s$ is the displacement vector and $\delta\boldsymbol{u}_\tau$ the relative variations. N stands for the number of terms of the expansion. According to Einstein's notation, the repeated subscript τ and s indicate summation.

In this paper, N is assumed equal to 5. Therefore, the displacement field can be expressed as

$$u_x = f_1 u_{x_1} + f_2 u_{x_2} + f_3 u_{x_3} + f_4 u_{x_4} + f_5 u_{x_5}$$
$$u_y = f_1 u_{y_1} + f_2 u_{y_2} + f_3 u_{y_3} + f_4 u_{y_4} + f_5 u_{y_5}$$
$$u_z = f_1 u_{z_1} + f_2 u_{z_2} + f_3 u_{z_3} + f_4 u_{z_4} + f_5 u_{z_5} \quad \text{(3a-c)}$$

where $f_1, .., f_5$ are function of z. Carrera et. al. [21] present polynomial functions ($f_1 = 1, f_2 = z, f_3 = z^2, ...$). This paper presents 5 non-polynomial functions: sinusoidal function (sin), tangential function (tan), exponential function (exp), hyperbolic function ($sinh$) and modified sinusoidal function (sin^*), see Table 1.

2.3. Elastic stress-strain relation

The stress (σ^k) and the strain (ε^k) of the k[th] layer are grouped as follows:

$$\boldsymbol{\sigma}_p^k = \begin{bmatrix} \sigma_{xx}^k & \sigma_{yy}^k & \sigma_{xy}^k \end{bmatrix}^T$$
$$\boldsymbol{\sigma}_n^k = \begin{bmatrix} \sigma_{xz}^k & \sigma_{yz}^k & \sigma_{zz}^k \end{bmatrix}^T$$
$$\boldsymbol{\varepsilon}_p^k = \begin{bmatrix} \varepsilon_{xx}^k & \varepsilon_{yy}^k & \varepsilon_{xy}^k \end{bmatrix}^T$$
$$\boldsymbol{\varepsilon}_n^k = \begin{bmatrix} \varepsilon_{xz}^k & \varepsilon_{yz}^k & \varepsilon_{zz}^k \end{bmatrix}^T \quad \text{(4a-d)}$$

Subscript "n" is related to the in-plane components, while "p" to the out-of-plane components. The strain-displacement relationship is:

$$\boldsymbol{\varepsilon}_p^k = \boldsymbol{D}_p \boldsymbol{u}^k \quad \text{(5a)}$$
$$\boldsymbol{\varepsilon}_n^k = \boldsymbol{D}_n \boldsymbol{u}^k = \left(\boldsymbol{D}_{np} + \boldsymbol{D}_{nz}\right)\boldsymbol{u}^k \quad \text{(5b)}$$

$$\boldsymbol{D}_p = \begin{bmatrix} \frac{\partial}{\partial x} & 0 & 0 \\ 0 & \frac{\partial}{\partial y} & 0 \\ \frac{\partial}{\partial y} & \frac{\partial}{\partial x} & 0 \end{bmatrix}, \quad \boldsymbol{D}_{np} = \begin{bmatrix} 0 & 0 & \frac{\partial}{\partial x} \\ 0 & 0 & \frac{\partial}{\partial y} \\ 0 & 0 & 0 \end{bmatrix}, \quad \boldsymbol{D}_{nz} = \begin{bmatrix} \frac{\partial}{\partial z} & 0 & 0 \\ 0 & \frac{\partial}{\partial z} & 0 \\ 0 & 0 & \frac{\partial}{\partial z} \end{bmatrix} \quad \text{(5c)}$$

For FGPs, the stress-strain relationship of the k[th] layer can be expressed as:

$$\begin{bmatrix}\sigma_{xx}^k\\ \sigma_{yy}^k\\ \sigma_{xy}^k\\ \sigma_{xz}^k\\ \sigma_{yz}^k\\ \sigma_{zz}^k\end{bmatrix}=\begin{bmatrix}C_{11}^k(z) & C_{12}^k(z) & 0 & 0 & 0 & C_{13}^k(z)\\ C_{12}^k(z) & C_{22}^k(z) & 0 & 0 & 0 & C_{23}^k(z)\\ 0 & 0 & C_{66}^k(z) & 0 & 0 & C_{36}^k(z)\\ 0 & 0 & 0 & C_{55}^k(z) & 0 & 0\\ 0 & 0 & 0 & 0 & C_{44}^k(z) & 0\\ C_{13}^k(z) & C_{23}^k(z) & C_{36}^k(z) & 0 & 0 & C_{33}^k(z)\end{bmatrix}\begin{bmatrix}\varepsilon_{xx}^k\\ \varepsilon_{yy}^k\\ \varepsilon_{xy}^k\\ \varepsilon_{xz}^k\\ \varepsilon_{yz}^k\\ \varepsilon_{zz}^k\end{bmatrix} \quad (6)$$

The C_{ij}^k expressions are given below:

$$C_{11}^k = C_{22}^k = C_{33}^k = \frac{E(z)(1-\nu)}{(1-2\nu)(1+\nu)}$$

$$C_{13}^k = C_{23}^k = C_{36}^k = \frac{E(z)\nu}{(1-2\nu)(1+\nu)}$$

$$C_{55}^k = C_{44}^k = C_{66}^k = \frac{E(z)}{2(1+\nu)} \quad (7a\text{-}c)$$

According to Eqs. (4a -d), the previous equation becomes:

$$\boldsymbol{\sigma}_p^k = \boldsymbol{C}_{pp}^k\boldsymbol{\varepsilon}_p^k + \boldsymbol{C}_{pn}^k\boldsymbol{\varepsilon}_n^k$$

$$\boldsymbol{\sigma}_n^k = \boldsymbol{C}_{np}^k\boldsymbol{\varepsilon}_p^k + \boldsymbol{C}_{nn}^k\boldsymbol{\varepsilon}_n^k \quad (8a\text{-}b)$$

where:

$$\boldsymbol{C}_{pp}^k = \begin{bmatrix}C_{11}^k & C_{12}^k & 0\\ C_{12}^k & C_{22}^k & 0\\ 0 & 0 & C_{66}^k\end{bmatrix}^k$$

$$\boldsymbol{C}_{nn}^k = \begin{bmatrix}C_{55}^k & 0 & 0\\ 0 & C_{44}^k & 0\\ 0 & 0 & C_{33}^k\end{bmatrix}^k$$

$$\boldsymbol{C}_{np}^k = \begin{bmatrix}0 & 0 & 0\\ 0 & 0 & 0\\ C_{13}^k & C_{23}^k & C_{36}^k\end{bmatrix}^k$$

$$\boldsymbol{C}_{pn}^k = \begin{bmatrix}0 & 0 & C_{13}^k\\ 0 & 0 & C_{23}^k\\ 0 & 0 & C_{36}^k\end{bmatrix}^k \quad (9a\text{-}d)$$

2.4. Principle of virtual works

Considering the static version of the principle of virtual work, the following expressions can be obtained:

$$\sum_{k=1}^{N_l} \int_{\Omega_k} \int_{A_k} \left\{ \delta \boldsymbol{\varepsilon}_p^{k\,T} \boldsymbol{\sigma}_p^k + \delta \boldsymbol{\varepsilon}_n^{k\,T} \boldsymbol{\sigma}_n^k \right\} d\Omega_k dz = \sum_{k=1}^{N_l} \delta L_e^k \tag{10}$$

where $\boldsymbol{\varepsilon}_p^k$ or $\boldsymbol{\sigma}_p^k$ are the stress and the strain vectors of the kth layer, N_l stands for number of layer and δL_e^k is the external virtual work.

Using Eqs. (8a-b), (5a-b) for a generic layer k, the Eq. (10) becomes:

$$\begin{aligned} \int_{\Omega_k} \int_{A_k} \Big\{ & (\boldsymbol{D}_p \delta \boldsymbol{u}^k)^T \left[\boldsymbol{C}_{pp}^k \boldsymbol{D}_p + \boldsymbol{C}_{pn}^k (\boldsymbol{D}_{np} + \boldsymbol{D}_{nz}) \right] \boldsymbol{u}^k \\ & + \left[(\boldsymbol{D}_{np} + \boldsymbol{D}_{nz}) \delta \boldsymbol{u}^k \right]^T \left[\boldsymbol{C}_{np}^k \boldsymbol{D}_p + \boldsymbol{C}_{nn}^k (\boldsymbol{D}_{np} + \boldsymbol{D}_{nz}) \right] \boldsymbol{u}^k \Big\} d\Omega_k dz = \delta L_e^k \end{aligned} \tag{11}$$

Using Eqs. (2.a.) and (2.b) into Eq. (11), the following expression can be obtained

$$\begin{aligned} \int_{\Omega_k} \int_{A_k} \Big\{ & \left(\boldsymbol{D}_p \delta \boldsymbol{u}_\tau^{\boldsymbol{k}} \right)^T \left(F_\tau F_s \boldsymbol{C}_{pp}^k \boldsymbol{D}_p \boldsymbol{u}_s^{\boldsymbol{k}} + F_\tau F_s \boldsymbol{C}_{pn}^k \boldsymbol{D}_{np} \boldsymbol{u}_s^{\boldsymbol{k}} + F_\tau F_{s_{,z}} \boldsymbol{C}_{pn}^k \boldsymbol{u}_s^{\boldsymbol{k}} \right) \\ & + \left(\boldsymbol{D}_{np} \delta \boldsymbol{u}_\tau^{\boldsymbol{k}} \right)^T \left[F_\tau F_s \boldsymbol{C}_{np}^k \boldsymbol{D}_p \boldsymbol{u}_s^{\boldsymbol{k}} + F_\tau F_s \boldsymbol{C}_{nn}^k \boldsymbol{D}_{np} \boldsymbol{u}_s^{\boldsymbol{k}} + F_\tau F_{s_{,z}} \boldsymbol{C}_{nn}^k \boldsymbol{u}_s^{\boldsymbol{k}} \right] \\ & + \left(\delta \boldsymbol{u}_\tau^{\boldsymbol{k}} \right)^T \left[F_{\tau_{,z}} F_s \boldsymbol{C}_{np}^k \boldsymbol{D}_p \boldsymbol{u}_s^{\boldsymbol{k}} + F_{\tau_{,z}} F_s \boldsymbol{C}_{nn}^k \boldsymbol{D}_{np} \boldsymbol{u}_s^{\boldsymbol{k}} + F_{\tau_{,z}} F_{s_{,z}} \boldsymbol{C}_{nn}^k \boldsymbol{u}_s^{\boldsymbol{k}} \right] \Big\} d\Omega_k dz \\ & = \delta L_e^k \end{aligned} \tag{12}$$

where the subscript z indicates partial derivative with respect to z. For simplicity, the following notations were introduced:

$$\boldsymbol{E}_{\tau spp}^k, \boldsymbol{E}_{\tau spn}^k, \boldsymbol{E}_{\tau s_{,z} pn}^k = \int_{A_k} (F_\tau F_s \boldsymbol{C}_{pp}^k, F_\tau F_s \boldsymbol{C}_{pn}^k, F_\tau F_{s_{,z}} \boldsymbol{C}_{pn}^k) dz$$

$$\boldsymbol{E}_{\tau snp}^k, \boldsymbol{E}_{\tau snn}^k \boldsymbol{E}_{\tau s_{,z} nn}^k = \int_{A_k} (\, F_\tau F_s \boldsymbol{C}_{np}^k, F_\tau F_s \boldsymbol{C}_{nn}^k, F_\tau F_{s_{,z}} \boldsymbol{C}_{nn}^k) dz$$

$$\boldsymbol{E}_{\tau_{,z} snp}^k, \boldsymbol{E}_{\tau_{,z} snn}^k, \boldsymbol{E}_{\tau_{,z} s_{,z} nn}^k = \int_{A_k} (F_{\tau_{,z}} F_s \boldsymbol{C}_{np}^k, F_{\tau_{,z}} F_s \boldsymbol{C}_{nn}^k, F_{\tau_{,z}} F_{s_{,z}} \boldsymbol{C}_{nn}^k) dz \tag{13}$$

The Eq. (12) becomes:

$$\int_{\Omega_k} \Big\{ \big(\boldsymbol{D}_p \delta \boldsymbol{u}_\tau^k\big)^T \big(\boldsymbol{E}_{\tau spp}^k \boldsymbol{D}_p \boldsymbol{u}_s^k + \boldsymbol{E}_{\tau spn}^k \boldsymbol{D}_{np} \boldsymbol{u}_s^k + \boldsymbol{E}_{\tau s_{,z} pn}^k \boldsymbol{u}_s^k\big) + \big(\boldsymbol{D}_{np} \delta \boldsymbol{u}_\tau^{\boldsymbol{k}}\big)^T \big(\boldsymbol{E}_{\tau snp}^k \boldsymbol{D}_p \boldsymbol{u}_s^{\boldsymbol{k}} + \boldsymbol{E}_{\tau snn}^k \boldsymbol{D}_{np} \boldsymbol{u}_s^{\boldsymbol{k}} + \boldsymbol{E}_{\tau s_{,z} nn}^k \boldsymbol{u}_s^k\big) + \big(\delta \boldsymbol{u}_\tau^{\boldsymbol{k}}\big)^T \big(\boldsymbol{E}_{\tau_{,z} snp}^k \boldsymbol{D}_p \boldsymbol{u}_s^{\boldsymbol{k}} + \boldsymbol{E}_{\tau_{,z} snn}^k \boldsymbol{D}_{np} \boldsymbol{u}_s^{\boldsymbol{k}} + \boldsymbol{E}_{\tau_{,z} s_{,z} nn}^k \boldsymbol{u}_s^{\boldsymbol{k}}\big) \Big\} d\Omega_k = \delta L_e^k \tag{14}$$

The integration by parts is applied at this point:

$$\int_{\Omega_k} (\boldsymbol{D}_\Omega \delta \boldsymbol{a}_\tau^k)^T \boldsymbol{a}_s^k \, d\Omega_k = -\int_{\Omega_k} \delta \boldsymbol{a}_\tau^{k\,T} \big(\boldsymbol{D}_\Omega{}^T \boldsymbol{a}_s^k\big) \, d\Omega_k + \int_{\Gamma_k} \delta \boldsymbol{a}_\tau^{k\,T} \big(\boldsymbol{I}_\Omega{}^T \boldsymbol{a}_s^k\big) \, d\Gamma \tag{15}$$

where $\Omega = p, np$. Applying the integrals by parts as in Eq. (15), Eq. (14) becomes:

$$\int_{\Omega_k} \Big\{ \big(\delta \boldsymbol{u}_\tau^k\big)^T \boldsymbol{K}_d^{k\tau s} \boldsymbol{u}_s^k \Big\} \, d\Omega_k + \int_{\Gamma_k} \Big\{ \big(\delta \boldsymbol{u}_\tau^k\big)^T \boldsymbol{\Pi}_d^{k\tau s} \boldsymbol{u}_s^k \Big\} \, d\Gamma_k = \int_{\Omega_k} \Big\{ \big(\delta \boldsymbol{u}_\tau^k\big)^T \boldsymbol{P}_s^k \Big\} d\Omega_k \tag{16}$$

where:

$$\boldsymbol{K}_d^{k\tau s} = \big(\boldsymbol{D}_p\big)^T \big[\boldsymbol{E}_{\tau spp}^k \boldsymbol{D}_p + \boldsymbol{E}_{\tau spn}^k \boldsymbol{D}_{np} + \boldsymbol{E}_{\tau s_{,z} pn}^k\big] + \big(\boldsymbol{D}_{np}\big)^T \big[\boldsymbol{E}_{\tau snp}^k \boldsymbol{D}_p + \boldsymbol{E}_{\tau snn}^k \boldsymbol{D}_{np} + \boldsymbol{E}_{\tau s_{,z} nn}^k\big] + \big[\boldsymbol{E}_{\tau_{,z} snp}^k \boldsymbol{D}_p + \boldsymbol{E}_{\tau_{,z} snn}^k \boldsymbol{D}_{np} + \boldsymbol{E}_{\tau_{,z} s_{,z} nn}^k\big] \tag{17a}$$

$$\boldsymbol{\Pi}_d^{k\tau s} = \big(\boldsymbol{I}_p^k\big)^{\boldsymbol{T}} \big[\boldsymbol{E}_{\tau spp}^k \boldsymbol{D}_p + \boldsymbol{E}_{\tau spn}^k \boldsymbol{D}_{np} + \boldsymbol{E}_{\tau s_{,z} pn}^k\big] + \big(\boldsymbol{I}_{np}^k\big)^T \big[\boldsymbol{E}_{\tau snp}^k \boldsymbol{D}_p + \boldsymbol{E}_{\tau snn}^k \boldsymbol{D}_{np} + \boldsymbol{E}_{\tau s_{,z} nn}^k\big] \tag{17b}$$

$$\boldsymbol{P}_s^k = \begin{bmatrix} 0 & 0 & \bar{F}_\tau q_{z(x,y)} \end{bmatrix}^T, \qquad \bar{F}_\tau = F_{\tau(z=h/2)} \tag{17c}$$

$$\boldsymbol{I}_p^k = \begin{bmatrix} n_1 & 0 & 0 \\ 0 & n_1 & 0 \\ n_2 & n_1 & 0 \end{bmatrix} \tag{17d}$$

$$\boldsymbol{I}_{np}^k = \begin{bmatrix} 0 & 0 & n_1 \\ 0 & 0 & n_2 \\ 0 & 0 & 0 \end{bmatrix} \tag{17e}$$

n_1 and n_2 are the components of the normal to the boundary Ω_k.

Finally, the governing equations are:

$$(\delta \boldsymbol{u}_{\tau}^{k})^{T}: \qquad \boldsymbol{K}_{d}^{k\tau s}\boldsymbol{u}_{s}^{k} = \boldsymbol{P}_{s}^{k} \tag{18}$$

With boundary condition stated as:

$$\boldsymbol{\Pi}_{d}^{k\tau s}\boldsymbol{u}_{s}^{k} = \boldsymbol{\Pi}_{d}^{k\tau s}\overline{\boldsymbol{u}}_{s}^{k} \tag{19}$$

$\boldsymbol{P}_{s}^{k}$ is the external load. The fundamental nucleus, $\boldsymbol{K}_{d}^{k\tau s}$, is assembled trough the depicted indexes, τ and s, which consider the order of expansion in z for the displacement field. The superscript *k* denotes the assembling on the number of layers.

3. Analytical Solution

Navier-type closed-form solutions are possible for simply supported plates. The displacement variable and the transverse distributed load can be expressed in the following Fourier series:

$$u_{x_s}^{k} = \sum_{m,n} \left(U_{x_s}^{k}\right) cos(\alpha x_k)\, sin(\beta y_k)\,, \qquad 0 \le x \le a; 0 \le y \le b \tag{20a}$$

$$u_{y_s}^{k} = \sum_{m,n} \left(U_{y_s}^{k}\right) sin(\alpha x_k)\, cos(\beta y_k)\,, \qquad 0 \le x \le a; 0 \le y \le b \tag{20b}$$

$$u_{z_s}^{k} = \sum_{m,n} \left(U_{z_s}^{k}\right) sin(\alpha x_k)\, sin(\beta y_k)\,, \qquad 0 \le x \le a; 0 \le y \le b \tag{20c}$$

$$q_z = \sum_{m,n} (Q_z)\, sin(\alpha x_k)\, sin(\beta y_k)\,, \qquad 0 \le x \le a; 0 \le y \le b \tag{20d}$$

$$\alpha = \frac{m\pi}{a_k}, \qquad \beta = \frac{n\pi}{b_k} \tag{20e}$$

where $U_{x_s}^{k}, U_{y_s}^{k}, U_{z_s}^{k}$ and Q_z are amplitudes, m and n are the number of waves, a_k and b_k are the dimensions of the plate.

Therefore the governing equation (18) becomes:

$$\begin{bmatrix} \overline{K}_{11} & \overline{K}_{12} & \overline{K}_{13} \\ \overline{K}_{21} & \overline{K}_{22} & \overline{K}_{23} \\ \overline{K}_{31} & \overline{K}_{32} & \overline{K}_{33} \end{bmatrix} \begin{bmatrix} U_{x_s}^{k} \\ U_{y_s}^{k} \\ U_{z_s}^{k} \end{bmatrix} = \begin{bmatrix} 0 \\ 0 \\ \overline{F}_s Q_z \end{bmatrix} \tag{21}$$

where:

$$\bar{K}_{11} = \int_z \left(C_{55}F_{\tau,z}F_{s,z} + \alpha^2 C_{11}F_\tau F_s + \beta^2 C_{66}F_\tau F_s\right)dz \quad (22a)$$

$$\bar{K}_{12} = \int_z (\alpha\beta C_{12}F_\tau F_s + \alpha\beta C_{66}F_\tau F_s)dz \quad (22b)$$

$$\bar{K}_{13} = \int_z \left(-\alpha C_{13}F_\tau F_{s,z} + \alpha C_{55}F_{\tau,z}F_s\right)dz \quad (22c)$$

$$\bar{K}_{21} = \int_z (\alpha\beta C_{12}F_\tau F_s + \alpha\beta C_{66}F_\tau F_s)dz \quad (22d)$$

$$\bar{K}_{22} = \int_z \left(C_{44}F_{\tau,z}F_{s,z} + \beta^2 C_{22}F_\tau F_s + \alpha^2 C_{66}F_\tau F_s\right)dz \quad (22e)$$

$$\bar{K}_{23} = \int_z \left(-\beta C_{23}F_\tau F_{s,z} + \beta C_{44}F_{\tau,z}F_s\right)dz \quad (22f)$$

$$\bar{K}_{31} = \int_z \left(\alpha C_{55}F_\tau F_{s,z} - \alpha C_{13}F_{\tau,z}F_s\right)dz \quad (22g)$$

$$\bar{K}_{32} = \int_z \left(\beta C_{44}F_\tau F_{s,z} - \beta C_{23}F_{\tau,z}F_s\right)dz \quad (22h)$$

$$\bar{K}_{33} = \int_z \left(C_{33}F_{\tau,z}F_{s,z} + \beta^2 C_{44}F_\tau F_s + \alpha^2 C_{55}F_\tau F_s\right)dz \quad (22i)$$

4. Numerical results and discussions

The bending analysis of simple supported FGPs is presented in what follow. Several and non-existent displacement fields under the CUF platform are developed for two kinds of FGPs (type A and type B) subjected to bi-sinusoidal load, $q_z = (Q_z)\,sin(\alpha x)\,sin(\beta y)$, on the top face ($z = h/2$) with $Q_z = 1$, $\alpha = \pi/a$ and $\beta = \pi/b$. Both types of FGPs are composed for two different materials whose properties are listed in the Table 2. Numerical examples are presented with various exponents, *p*, of the Eqs. (1b and 1c) and several values of the side-to-thickness ratio, a/h. For this study the following relations for the non-dimensional deflection and stresses were utilized:

$$\bar{w} = w\left(\frac{a}{2}, \frac{b}{2}, z\right)\frac{10h^3E}{q_0a^4}, \bar{u} = w\left(0, \frac{b}{2}, z\right)\frac{10h^3E}{q_0a^4}, \bar{\sigma}_{xx} = \sigma_{xx}\left(\frac{a}{2}, \frac{b}{2}, z\right)\frac{h}{q_0a}$$

$$\bar{\sigma}_{xz} = \sigma_{xz}\left(0, \frac{b}{2}, z\right)\frac{h}{q_0a}, \bar{\sigma}_{zz} = \sigma_{xz}\left(\frac{a}{2}, \frac{b}{2}, z\right)\frac{h}{q_0a}, \bar{\sigma}_{xy} = \sigma_{xy}(0,0,z)\frac{h}{q_0a} \quad \text{(23a-f)}$$

4.1. Analysis of type A FGPs.

In this example, an FG square plate of type A is considered. This plate is graded across to the thickness from Alumina (ceramic material) on the top to Aluminum (metal material) on the bottom according the Eqs. (1a-b). Properties of the aluminum and the alumina are shown in Table 2.

Table 3 presents values of non-dimensional deflection $\bar{w}_{(z=0)}$ and $\bar{\sigma}_{xx_{(z=h/3)}}$ stresses of the five different displacement fields under CUF for various values of the exponent $p = \{0, 0.5, 1, 4, 10\}$ and the side-to-thickness ratio $a/h = \{4, 10, 100\}$. The results are compared with the results by Carrera et al. [21] and Neves at el. [33]. The non-polynomial displacement fields, *sinh*, *sec*, and *exp*, give results matching those by Carrera et al. [21] for N=4. However the sinusoidal field (*sin*) presents different values. The displacement field, *sin**, is a modified sinusoidal field and presents close to *pol* results [21]. Figures 5 to 10 present the displacements and stresses across the thickness direction according to the present non-polynomial displacement fields (*sin*, *sinh*, *exp* and *tan*). Results are compared to those from polynomial (*pol*) fields for $p = \{1, 4, 10\}$ and $a/h = 4$.

Figures 11 to 16 show $\bar{\sigma}_{xz(0,b/2)}$ and $\bar{\sigma}_{zz(a/2,b/2)}$ from *sin*, *sin** and polynomial displacement fields. The difference between *sin** and *pol* results is minimal. A worse match was found in the case of *sin* for $p = \{1, 4, 10\}$ and $a/h = 4$.

Results suggest that the use of some terms in *sin* may be detrimental. A solution might be given by the mixed axiomatic/asymptotic approach that has been developed by Carrera [34,35]. Such an approach can evaluate the effectiveness of each term of an expansion and build the best theory for a given problem [36].

4.2. Analysis of type B FGPs

In this example, the FGPs of type B is composed of alumina at the top skin with thickness $h/10$, aluminum at the bottom skin with thickness $h/10$, and a core of FG with volume fraction according Eq. (1c). This square plate is simply supported under a bi-sinusoidal load.

Table 4 presents values of non-dimensional deflection $\overline{w}_{(z=0)}$ and $\bar{\sigma}_{xx\,(z=h/6)}$ stress in all displacement fields presented in this paper for various values for the side-of-thickness ratio $a/h = \{4, 10, 100\}$ and several values for exponent $p = \{0, 0.5, 1, 4, 10\}$. These results are compared with Carrera et al. [21] and Neves at el. [33]. As in the plate of type A, the results of *sin** are closer to polynomials CUF results presented by Carrera et al. [21] than *sin*. The sinusoidal displacement field present quite different results, therefore, the modified sinusoidal field, *sin**, was presented and compared with polynomial [21] results in Figures 23 to 28 for $p = \{1, 4, 10\}$ and $a/h = 100$.

5. Conclusions

This paper presents a static analysis for FG single and sandwich plates using Carrera's Unified Formulation (N=4) with five different and non-existent displacement fields of the form non-polynomial (sinusoidal (sin), tangential (tan), exponential (exp), hyperbolic ($sinh$) and modified sinusoidal (sin^*)).

The displacements $\bar{u}$, $\overline{w}$ and the stresses σ_{xx}, σ_{xy} had a good agreement with the results of Carrera et. al. [21] (*pol*) for single and sandwich FGPs. However, the stresses σ_{zz} and σ_{xz} in the sinusoidal displacement field present different results.

Using a modified sinusoidal function (sin^*), the results were closer to (*pol*) than with (*sin*). This suggests that the displacement field sin could be further enhanced.

Acknowledgement

The Peruvian team of this paper would like to thanks to Professor Erasmo Carrera for give us the opportunity to work with his prestigious team in the beginning of the present year (2015).

References

[1] Koizumi M. The concept of FGM Ceramic transactions. Funct Grad Mater 1993;34:3-10

[2] Thai HT, Kim SE. A review of theories for the modeling ad analysis of functionally graded plates and shells. Compos Struct 2015;128:70-86.

[3] Swaminathan K, Naveenkumar DT, Zenkour AM, Carrera E. Stress, vibration and buckling analysis of FGM plates – A state-of-art review. Compos Struct 2015;120:10-31.

[4] Demasi L. ∞6 mixed plate theories based on the generalized unified formulation Part I: Governing Equations. Compos Struct 2009;87:1–11.

[5] Demasi L. ∞6 mixed plate theories based on the generalized unified formulation. Part II: Layerwise theories. Compos Struct 2009;87:12–22.

[6] Demasi L. ∞6 mixed plate theories based on the generalized unified formulation. Part III: Advanced mixed high order shear deformation theories. Compos Struct 2009;87:183–94.

[7] Demasi L.∞6 mixed plate theories based on the generalized unified formulation. Part IV: Zig–zag theories. Compos Struct 2009;87:195–205.

[8] Demasi L. ∞6 mixed plate theories based on the generalized unified formulation. Part V: Results. Compos Struct 2009;88:1–16.

[9] Reddy JN, Liu CF. A higher-order shear of deformation theory of laminated elastic shells. Int J Eng Sci 1985;23:319-30

[10] Reddy JN. Analysis of functionally graded plates. Int J Numer Meth Eng 2000;47:663–84.

[11] Touratier M. An efficient standard plate theory. Int J Eng Sci 1991;29 (8):901–16.

[12] Soldatos KP. A transverse shear deformation theory for homogeneous monoclinic plates. Acta Mech 1992;94:195–220.

[13] Zenkour AM. Generalized shear deformation theory for bending analysis of functionally graded plates. Appl Math Model 2006;30:67–84.

[14] Zenkour AM. Benchmark trigonometric and 3-D elasticity solutions for an exponentially graded thick rectangular plate. Appl Math Model 2007;77:197–214

[15] Karama M. Mechanical behavior or laminated composite beam by the new multilayer laminated composite structures model with transverse shear stress continuity. Acta Mech 2003;40:1525-46.

[16] Mantari JL, Oktem AS, Guedes Soares C. Bending response of functionally graded plates by using a new higher order shear deformation theory. Compos Struct 2012;94:714–23.

[17] Mantari JL, Oktem AS, Guedes Soares C. Static and dynamic analysis of laminated composite and sandwich plates and shells by using a new higherorder shear deformation theory. Compos Struct 2011;94:37–49.

[18] Mantari JL, Oktem AS, Guedes Soares C. A new trigonometric deformation theory for isotropic, laminated composite and sandwich plates. Int J Solids Struct 2012;49:43–53.

[19] Mantari JL, Guedes Soares C. Bending analysis of thick exponentially graded plates using a new trigonometric higher order shear deformation theory.Compos Struct 2012;94:1991–2000.

[20] Mantari JL, Granados EV, Guedes Soares C. Vibrational analysis of advanced composite plates resting on elastic foundation.

[21] Carrera E, Brishetto S, Cinefra M, Soave M. Effects of thickness stretching in functionally graded plates and shells. Compos Part B: Eng 2011;42(2):123-33

[22] Carrera E. Evaluation of layer-wise mixed theories for laminated plate analysis. AIAA J 1998(36):830-9.

[23] Carrera E. Developments, ideas, and evaluations based upon reissner's mixed variational theorem in the modelling of multilayered plates and shells. Appl Mech Rev 2001;54:301–29.

[24] Carrera Erasmo. Theories and finite elements for multilayered plates and shells: a unified compact formulation with numerical assessment and benchmarking. Arch Comput Methods Eng 2003;10:215–96.

[25] Brischetto S, Carrera E. Advanced mixed theories for bending analysis of functionally graded plates. Comput Struct 2010;88(23–24):1474–83.

[26] Cinefra M, Belouettar S, Soave M, Carrera E. Variable kinematic models applied to free-vibration analysis of functionally graded material shells. European Journal of Mechanics A/Solids 2010;29:1078-1087.

[27] Carrera E, Brischetto S, Robaldo A. Variable kinematic model for the analysis of functionally graded material plates. AIAA J 2008;46:194–203.

[28] Ferreira AJM, Carrera E, Cinefra M, Roque CMC, Polit O. Analysis of laminated shells by a sinusoidal shear deformation theory and radial basis functions

collocation, accounting for through-the-thickness deformations. Compos B Eng 2011;42(5):1276–84.

[29] Neves AMA, Ferreira AJM, Carrera E, Roque CMC, Cinefra M, Jorge RMN, et al. Bending of FGM plates by a sinusoidal plate formulation and collocation with radial basis functions. Mech Res Commun 2011;38(5):368–71.

[30] Neves AMA, Ferreira AJM, Carrera E, Roque CMC, Cinefra M, Jorge RMN, et al. A quasi-3D sinusoidal shear deformation theory for the static and free vibration analysis of functionally graded plates. Compos B Eng 2012;43(2):711–25.

[31] Neves AMA, Ferreira AJM, Carrera E, Cinefra M, Roque CMC, Jorge RMN, et al. A quasi-3D hyperbolic shear deformation theory for the static and free vibration analysis of functionally graded plates. Compos Struct 2012;94(5):1814–25.

[32] Neves AMA, Ferreira AJM, Carrera E, Cinefra M, Jorge RMN, Soares CMM. Buckling analysis of sandwich plates with functionally graded skins using anew quasi-3D hyperbolic sine shear deformation theory and collocation with radial basis function. ZAMM – J Appl Match Mech/Z Angew Match Mech 2012;92(9):749-66.

[33] Neves AMA, Ferreira AJM, Carrera E, Cinefra M, Jorge RMN, Soares CMM. Static, free vibration and buckling analysis of isotropic and sandwich functionally graded plates using a quasi-3D higher-order shear deformation theory and a meshless technique. Compos Part B: Eng 2013;44(1):657-74

[34] Carrera E, Petrolo M. Guidelines and recommendation to construct theories for metallic and composite plates. AIAA Journal 2010; 12: 2852-2866

[35] Carrera E, Petrolo M. On the effectiveness of higher-order terms in refined beam theories. Journal of Applied Mechanics 2011.

[36] Carrera E, Cinefra M, Petrolo M, Lamberti A. Results on best theories for metallic and laminated shells including Layer-Wise models. Composite Structures 2015; 126: 285-298.

Table Legends

Table 1. Thickness functions.

Table 2. Properties of materials.

Table 3. Non-dimensional stress $\bar{\sigma}_{xx(h/3)}$ and deflection $\bar{w}_{(0)}$ of Type A square plate under bi-sinusoidal transverse load.

Table 4. Non-dimensional stress $\bar{\sigma}_{xx(h/6)}$ and deflection $\bar{w}_{(0)}$ of Type B square plate under bi-sinusoidal transverse load.

Figure Captions

Figure 1. Geometry of functionally graded single plate (Type-A)

Figure 2. Geometry of functionally graded sandwich plate (Type-B)

Figure 3. V_c along the thickness of a FG plate of Type-A for different values of "p".

Figure 4. V_c along the thickness of a FG plate of Type-B for different values of "p".

Figure 5. Dimensionless displacement ($\bar{u}$) through the thickness direction of a square plate type-A, a/h=4 and different values of *p* and several displacement fields.

Figure 6. Dimensionless stress ($\bar{\sigma}_{xx}$) through the thickness direction of a square plate type-A, a/h=4 and different values of *p* and several displacement fields..

Figure 7. Dimensionless stress ($\bar{\sigma}_{xy}$) through the thickness direction of a square plate type-A , a/h=4 and different values of *p* and several displacement fields.

Figure 8. Dimensionless stress ($\bar{\sigma}_{zz}$) through the thickness direction of a square plate type-A , a/h=4 and different values of *p* and several displacement fields.

Figure 9. Dimensionless stress ($\bar{\sigma}_{xz}$) through the thickness direction of a square plate type-A , a/h=4 and different values of *p* and several displacement fields.

Figure 10. Dimensionless displacement ($\bar{w}$) through the thickness direction of a square plate type-A , a/h=4 and different values of *p* and several displacement fields.

Figure 11. Dimensionless stress ($\bar{\sigma}_{xz}$) through the thickness direction for *sin*, *sin** and *pol* displacement field of a square plate type-A , a/h=4 and *p*=1.

Figure 12. Dimensionless stress ($\bar{\sigma}_{xz}$) through the thickness direction for *sin*, *sin** and *pol* displacement field of a square plate type-A , a/h=4 and *p*=4.

Figure 13. Dimensionless stress ($\bar{\sigma}_{xz}$) through the thickness direction for *sin*, *sin** and *pol* displacement field of a square plate type-A , a/h=4 and *p*=10.

Figure 14. Dimensionless stress ($\bar{\sigma}_{zz}$) through the thickness direction for *sin*, *sin** and *pol* displacement field of a square plate type-A , a/h=4 and *p*=1.

Figure 15. Dimensionless stress ($\bar{\sigma}_{zz}$) through the thickness direction for *sin*, *sin** and *pol* displacement field of a square plate type-A , a/h=4 and *p*=4.

Figure 16. Dimensionless stress ($\bar{\sigma}_{zz}$) through the thickness direction for *sin*, *sin** and *pol* displacement field of a square plate type-A , a/h=4 and *p*=10.

Figure 17. Dimensionless displacement ($\bar{u}$) through the thickness direction of a square plate type-B , a/h=100 and different values of *p* and several displacement fields.

Figure 18. Dimensionless stress ($\bar{\sigma}_{xx}$) through the thickness direction of a square plate type-B , a/h=100 and different values of *p* and several displacement fields.

Figure 19. Dimensionless stress ($\bar{\sigma}_{xy}$) through the thickness direction of a square plate type-B , a/h=100 and different values of *p* and several displacement fields.

Figure 20. Dimensionless stress ($\bar{\sigma}_{zz}$) through the thickness direction of a square plate type-B , a/h=100 and different values of *p* and several displacement fields.

Figure 21. Dimensionless stress ($\bar{\sigma}_{xz}$) through the thickness direction of a square plate type-B , a/h=100 and different values of *p* and several displacement fields.

Figure 22. Dimensionless displacement ($\bar{w}$) through the thickness direction of a square plate type-B , a/h=100 and different values of *p* and several displacement fields.

Figure 23. Dimensionless stress ($\bar{\sigma}_{xz}$) through the thickness direction for *sin*, *sin** and *pol* displacement field of a square plate type-B , a/h=100 and *p*=1.

Figure 24. Dimensionless stress ($\bar{\sigma}_{xz}$) through the thickness direction for *sin*, *sin** and *pol* displacement field of a square plate type-B , a/h=100 and *p*=4.

Figure 25. Dimensionless stress ($\bar{\sigma}_{xz}$) through the thickness direction for *sin*, *sin** and *pol* displacement field of a square plate type-B , a/h=100 and *p*=10.

Figure 26. Dimensionless stress ($\bar{\sigma}_{zz}$) through the thickness direction for *sin*, *sin** and *pol* displacement field of a square plate type-B , a/h=100 and *p*=1.

Figure 27. Dimensionless stress ($\bar{\sigma}_{zz}$) through the thickness direction for *sin*, *sin** and *pol* displacement field of a square plate type-B , a/h=100 and *p*=4.

Figure 28. Dimensionless stress ($\bar{\sigma}_{zz}$) through the thickness direction for *sin*, *sin** and *pol* displacement field of a square plate type-B , a/h=100 and *p*=10.

Tables

Table 1.

	$f_1(z)$	$f_2(z)$	$f_3(z)$	$f_4(z)$	$f_5(z)$
pol	1	z	z^2	z^3	z^4
sinh	1	z	$\cosh(z/h)$	$\sinh(z/h)$	$\cosh^2(z/h)$
exp	1	z	$e^{(z/h)^2}$	$ze^{(z/h)^2}$	$z^2e^{(z/h)^2}$
tan	1	z	$\sec(z/5h)$	$\mathrm{tg}(z/5h)$	$\sec^2(z/5h)$
sin	1	z	$\cos(z\pi/h)$	$\sin(z\pi/h)$	$\cos^2(z\pi/h)$
sin $*$	1	z	$\cos(z/h)$	$\sin(z/h)$	$\cos^2(z/h)$

Table 2.

Material	Properties	
	E(GPa)	ν
Aluminum (Al)	70	0.3
Alumina (Al_2O_3)	380	0.3

Table 3.

p	Theory	$\bar{\sigma}_{xx(h/3)}$			$\bar{w}_{(0)}$		
		a/h=4	a/h=10	a/h=100	a/h=4	a/h=10	a/h=100
0	Ref. [33] $\epsilon_{zz}\neq0$	0.5278	1.3176	13.1610	0.3665	0.2942	0.2803
0	Ref. [21] $\epsilon_{zz}\neq0$	0.5539	1.3278	13.1728	0.3663	0.2942	0.2804
0	**Present (sinh)**	**0.5540**	**1.3277**	**13.1723**	**0.3663**	**0.2942**	**0.2804**
0	**Present (exp)**	**0.5540**	**1.3271**	**13.1654**	**0.3663**	**0.2942**	**0.2804**
0	**Present (tan)**	**0.5539**	**1.3278**	**13.1728**	**0.3663**	**0.2942**	**0.2804**
0	**Present (sin)**	**0.5505**	**1.3207**	**13.1041**	**0.3661**	**0.2942**	**0.2804**
0	**Present (sin*)**	**0.5537**	**1.3276**	**13.1722**	**0.3663**	**0.2942**	**0.2804**
0.5	Ref. [33] $\epsilon_{zz}\neq0$	0.5860	1.4680	14.673	0.5493	0.4548	0.4365
0.5	Ref. [21] $\epsilon_{zz}\neq0$	0.6109	1.4746	14.6461	0.55320	0.4520	0.4325
0.5	**Present (sinh)**	**0.6110**	**1.4746**	**14.6454**	**0.55320**	**0.4520**	**0.4325**
0.5	**Present (exp)**	**0.6113**	**1.4738**	**14.6351**	**0.55320**	**0.4520**	**0.4325**
0.5	**Present (tan)**	**0.6109**	**1.4746**	**14.6461**	**0.55320**	**0.4520**	**0.4325**
0.5	**Present (sin)**	**0.6055**	**1.4640**	**14.5446**	**0.5530**	**0.4520**	**0.4325**
0.5	**Present (sin*)**	**0.6106**	**1.4745**	**14.6453**	**0.5532**	**0.4520**	**0.4325**
1	Ref. [33] $\epsilon_{zz}\neq0$	0.5911	1.4917	14.945	0.7020	0.5868	0.5647
1	Ref. [21] $\epsilon_{zz}\neq0$	0.6221	1.5064	14.9692	0.7171	0.5875	0.5625
1	**Present (sinh)**	**0.6223**	**1.5064**	**14.9683**	**0.7171**	**0.5875**	**0.5625**
1	**Present (exp)**	**0.6227**	**1.5056**	**14.9565**	**0.7172**	**0.5875**	**0.5625**
1	**Present (tan)**	**0.6221**	**1.5064**	**14.9692**	**0.7171**	**0.5875**	**0.5625**
1	**Present (sin)**	**0.6155**	**1.4937**	**14.8486**	**0.7168**	**0.5875**	**0.5625**
1	**Present (sin*)**	**0.6218**	**1.5062**	**14.9682**	**0.7171**	**0.5875**	**0.5625**
4	Ref. [33] $\epsilon_{zz}\neq0$	0.4330	1.1588	11.737	1.1108	0.8700	0.8240
4	Ref. [21] $\epsilon_{zz}\neq0$	0.4877	1.1971	11.9227	1.1585	0.8822	0.8287
4	**Present (sinh)**	**0.4880**	**1.1972**	**11.922**	**1.1585**	**0.8822**	**0.8287**
4	**Present (exp)**	**0.4897**	**1.1971**	**11.9133**	**1.1580**	**0.8821**	**0.8287**
4	**Present (tan)**	**0.4878**	**1.1972**	**11.9227**	**1.1585**	**0.8822**	**0.8287**
4	**Present (sin)**	**0.4801**	**1.1853**	**11.8179**	**1.1583**	**0.8822**	**0.8286**
4	**Present (sin*)**	**0.4874**	**1.1969**	**11.9219**	**1.1585**	**0.8822**	**0.8287**
10	Ref. [33] $\epsilon_{zz}\neq0$	0.3097	0.8462	8.6010	1.3334	0.9888	0.9227
10	Ref. [21] $\epsilon_{zz}\neq0$	0.3696	0.8966	8.9078	1.3745	1.0072	0.9362
10	**Present (sinh)**	**0.3700**	**0.8967**	**8.9074**	**1.3745**	**1.0072**	**0.9362**
10	**Present (exp)**	**0.3723**	**0.8972**	**8.9024**	**1.3737**	**1.0070**	**0.9362**
10	**Present (tan)**	**0.3697**	**0.8966**	**8.9078**	**1.3745**	**1.0072**	**0.9362**
10	**Present (sin)**	**0.3610**	**0.8875**	**8.8403**	**1.3744**	**1.0072**	**0.9361**
10	**Present (sin*)**	**0.3690**	**0.8963**	**8.9073**	**1.3746**	**1.0072**	**0.9362**

Table 4.

p	Theory	$\bar{\sigma}_{xx(h/6)}$			$\bar{w}_{(0)}$		
		a/h =4	a/h =10	a/h =100	a/h =4	a/h =10	a/h =100
0	Ref. [33] $\epsilon_{zz}\neq 0$	0.2208	0.2227	0.2228	0.4447	0.3711	0. 3568
0	Ref. [21] $\epsilon_{zz}\neq 0$	0.2395	0.2401	0.2403	0.4498	0.3728	0.3579
0	**Present (sinh)**	**0.2394**	**0.2400**	**0.2402**	**0.4498**	**0.3728**	**0.3579**
0	**Present (exp)**	**0.2383**	**0.2389**	**0.2391**	**0.4497**	**0.3728**	**0.3579**
0	**Present (tan)**	**0.2395**	**0.2401**	**0.2403**	**0.4498**	**0.3728**	**0.3579**
0	**Present (sin)**	**0.2405**	**0.2411**	**0.2412**	**0.4497**	**0.3728**	**0.3579**
0	**Present (sin*)**	**0.2397**	**0.2403**	**0.2405**	**0.4498**	**0.3728**	**0.3579**
0.5	Ref. [33] $\epsilon_{zz}\neq 0$	0.2546	0.2581	0.2585	0.6168	0.5238	0.5058
0.5	Ref. [21] $\epsilon_{zz}\neq 0$	0.2568	0.2565	0.2565	0.6258	0.5222	0.5023
0.5	**Present (sinh)**	**0.2566**	**0.2563**	**0.2563**	**0.6258**	**0.5222**	**0.5023**
0.5	**Present (exp)**	**0.2552**	**0.2550**	**0.2550**	**0.6258**	**0.5222**	**0.5023**
0.5	**Present (tan)**	**0.2567**	**0.2565**	**0.2565**	**0.6258**	**0.5222**	**0.5023**
0.5	**Present (sin)**	**0.2589**	**0.2586**	**0.2586**	**0.6257**	**0.5222**	**0.5022**
0.5	**Present (sin*)**	**0.2570**	**0.2567**	**0.2567**	**0.6258**	**0.5222**	**0.5023**
1	Ref. [33] $\epsilon_{zz}\neq 0$	0.2745	0.2789	0.2795	0.7417	0.6305	0.6092
1	Ref. [21] $\epsilon_{zz}\neq 0$	0.2604	0.2594	0.2593	0.7627	0.6325	0.6073
1	**Present (sinh)**	**0.2604**	**0.2594**	**0.2592**	**0.7627**	**0.6325**	**0.6073**
1	**Present (exp)**	**0.2595**	**0.2586**	**0.2584**	**0.7628**	**0.6325**	**0.6073**
1	**Present (tan)**	**0.2604**	**0.2594**	**0.2593**	**0.7627**	**0.6325**	**0.6073**
1	**Present (sin)**	**0.2618**	**0.2606**	**0.2604**	**0.7624**	**0.6324**	**0.6073**
1	**Present (sin*)**	**0.2605**	**0.2595**	**0.2593**	**0.7627**	**0.6325**	**0.6073**
4	Ref. [33] $\epsilon_{zz}\neq 0$	0.2696	0.2747	0.2753	1.0371	0.8199	0.7784
4	Ref. [21] $\epsilon_{zz}\neq 0$	0.2400	0.2398	0.2398	1.0930	0.8307	0.7797
4	**Present (sinh)**	**0.2402**	**0.2401**	**0.2401**	**1.0929**	**0.8307**	**0.7797**
4	**Present (exp)**	**0.2388**	**0.2386**	**0.2386**	**1.0922**	**0.8305**	**0.7797**
4	**Present (tan)**	**0.2400**	**0.2398**	**0.2398**	**1.0929**	**0.8307**	**0.7797**
4	**Present (sin)**	**0.2390**	**0.2384**	**0.2384**	**1.0931**	**0.8307**	**0.7797**
4	**Present (sin*)**	**0.2397**	**0.2395**	**0.2395**	**1.0930**	**0.8307**	**0.7797**
10	Ref. [33] $\epsilon_{zz}\neq 0$	0.1995	0.2034	0.2039	1.1752	0.8645	0.8050
10	Ref. [21] $\epsilon_{zz}\neq 0$	0.1932	0.1943	0.1946	1.2173	0.8741	0.8077
10	**Present (sinh)**	**0.1928**	**0.1938**	**0.1941**	**1.2171**	**0.8740**	**0.8077**
10	**Present (exp)**	**0.1893**	**0.1902**	**0.1904**	**1.2149**	**0.8736**	**0.8077**
10	**Present (tan)**	**0.1931**	**0.1942**	**0.1944**	**1.2172**	**0.8741**	**0.8077**
10	**Present (sin)**	**0.1990**	**0.2003**	**0.2006**	**1.2189**	**0.8744**	**0.8077**
10	**Present (sin*)**	**0.1937**	**0.1948**	**0.1951**	**1.2174**	**0.8741**	**0.8077**

Figures

Figure 1.

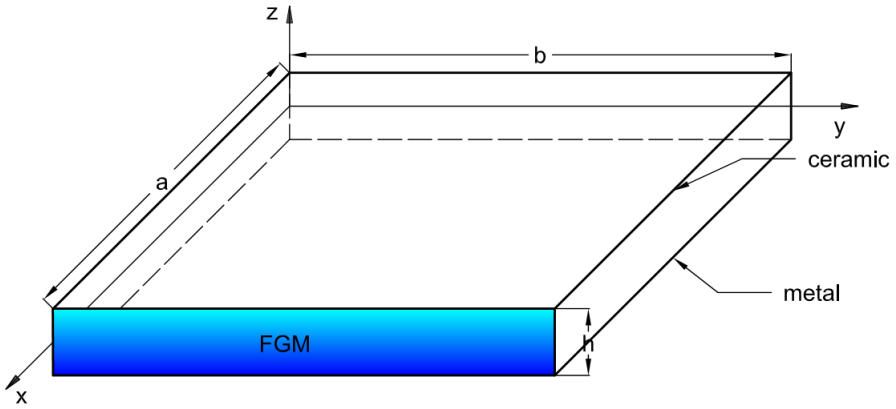

Figure 2.

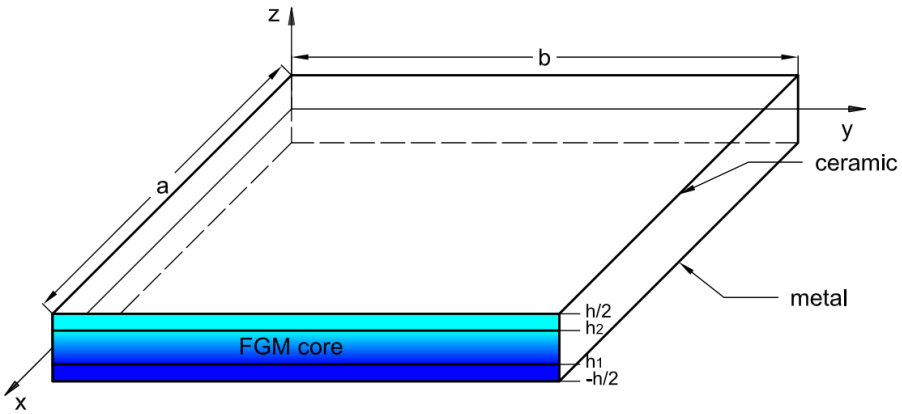

Figure 3.

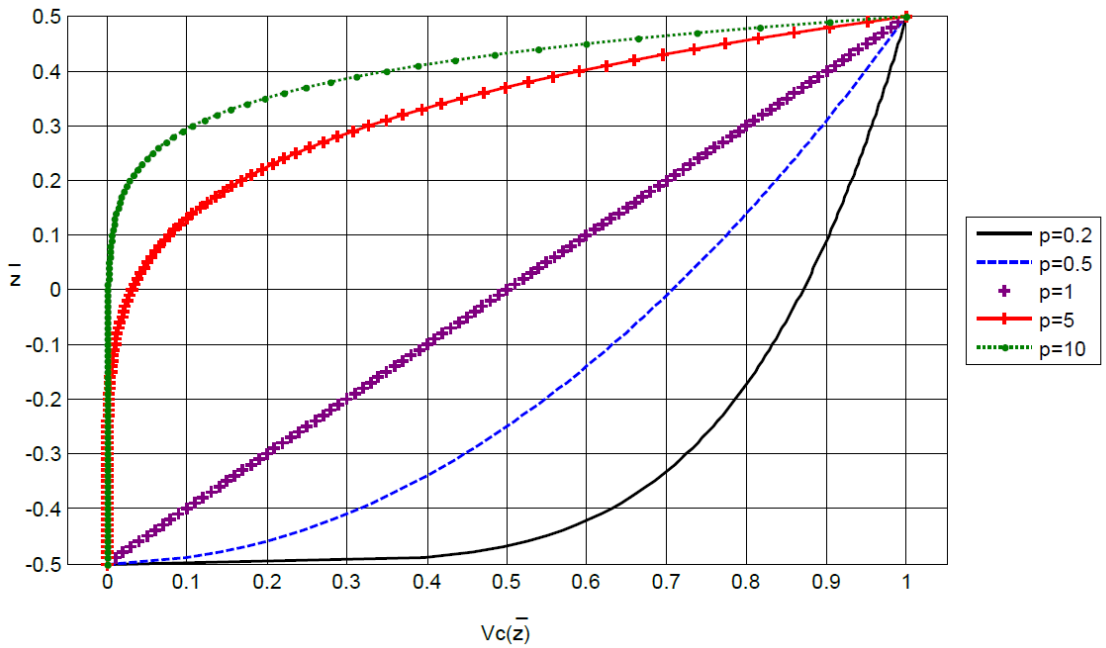

Figure 4.

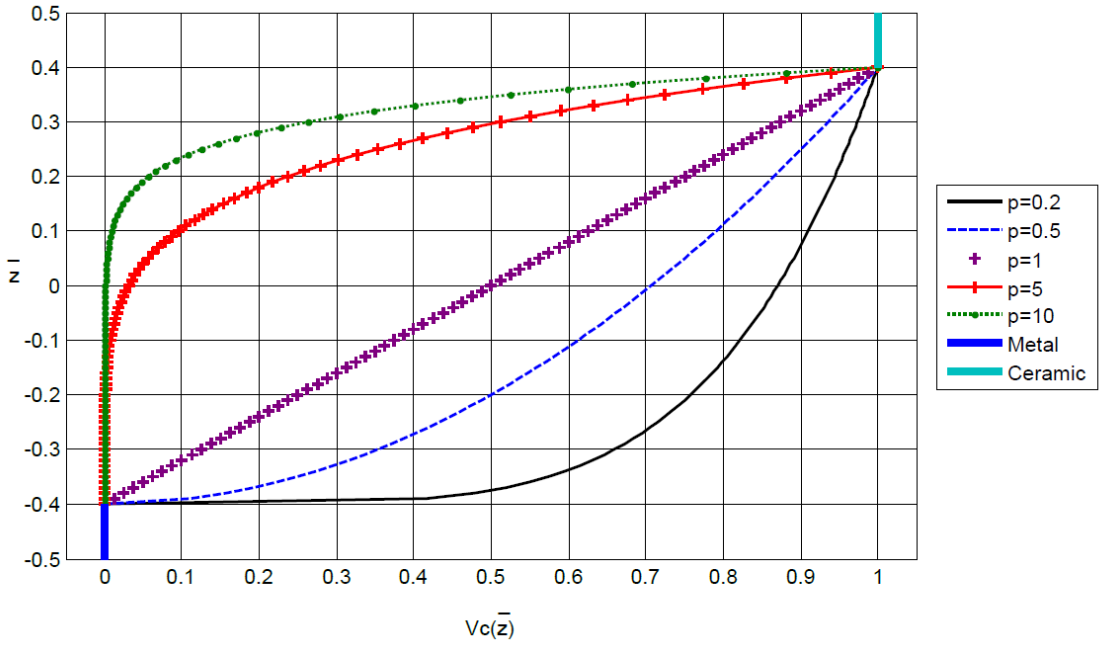

Figure 5.

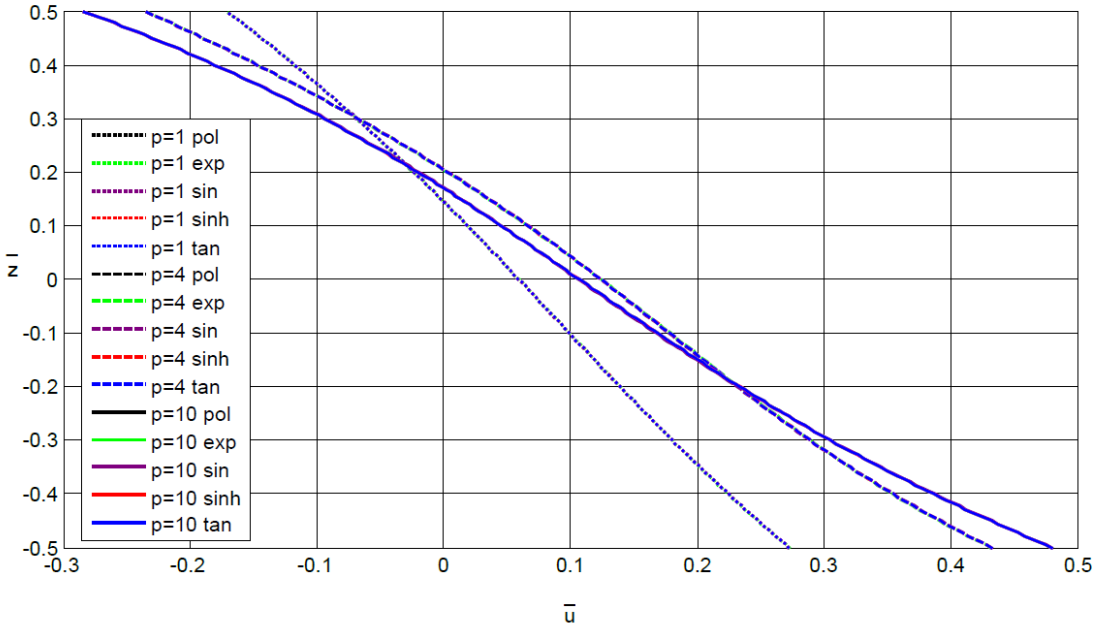

Figure 6.

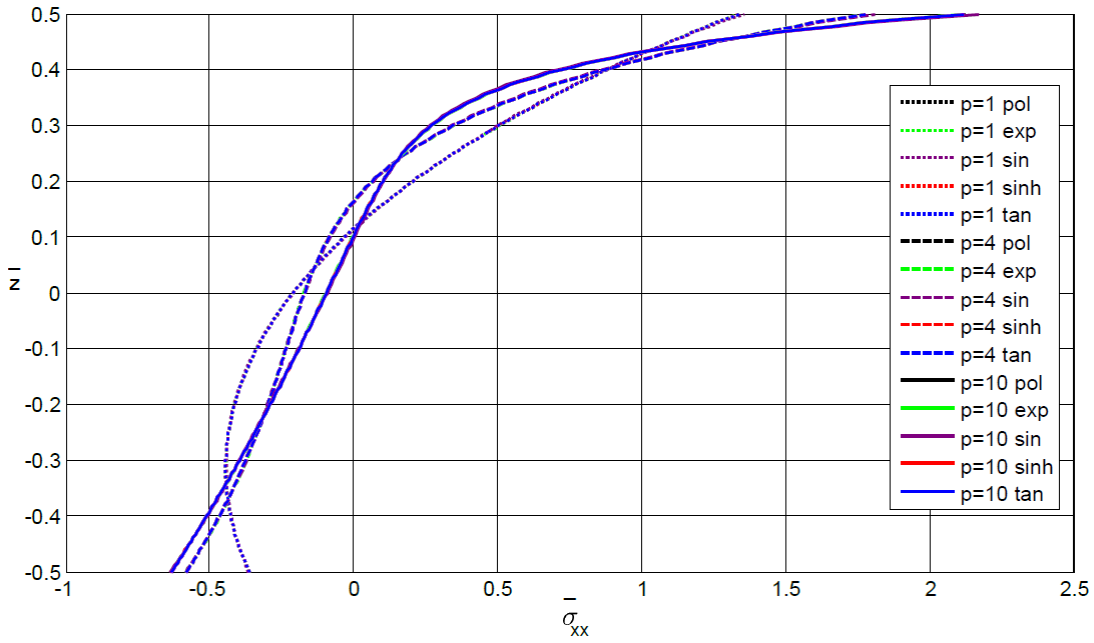

Figure 7.

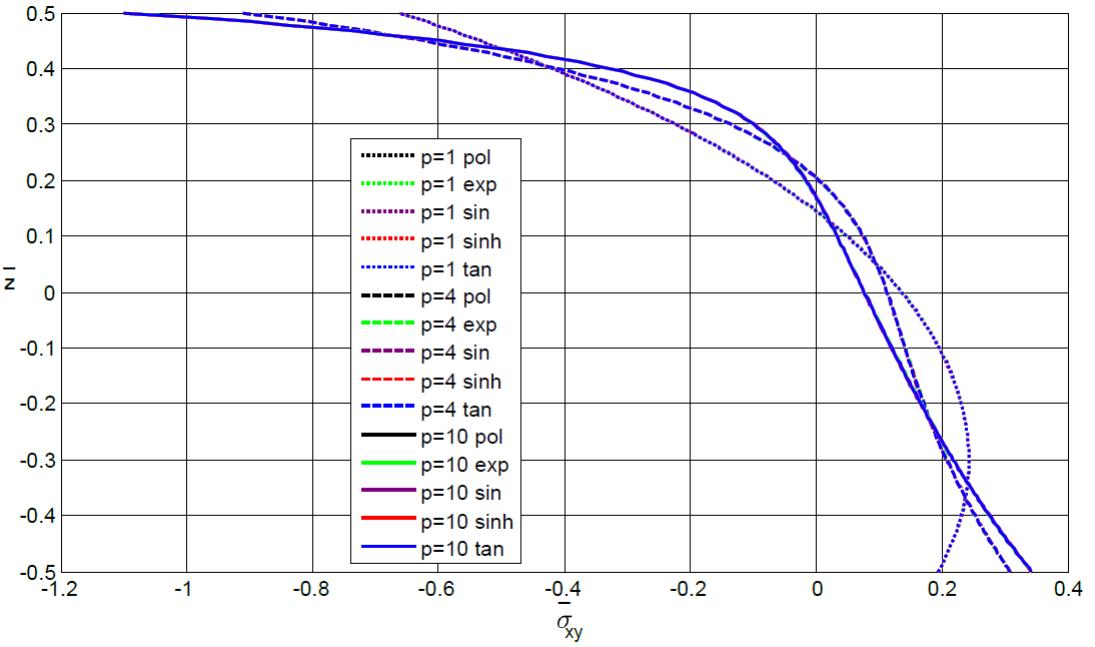

Figure 8.

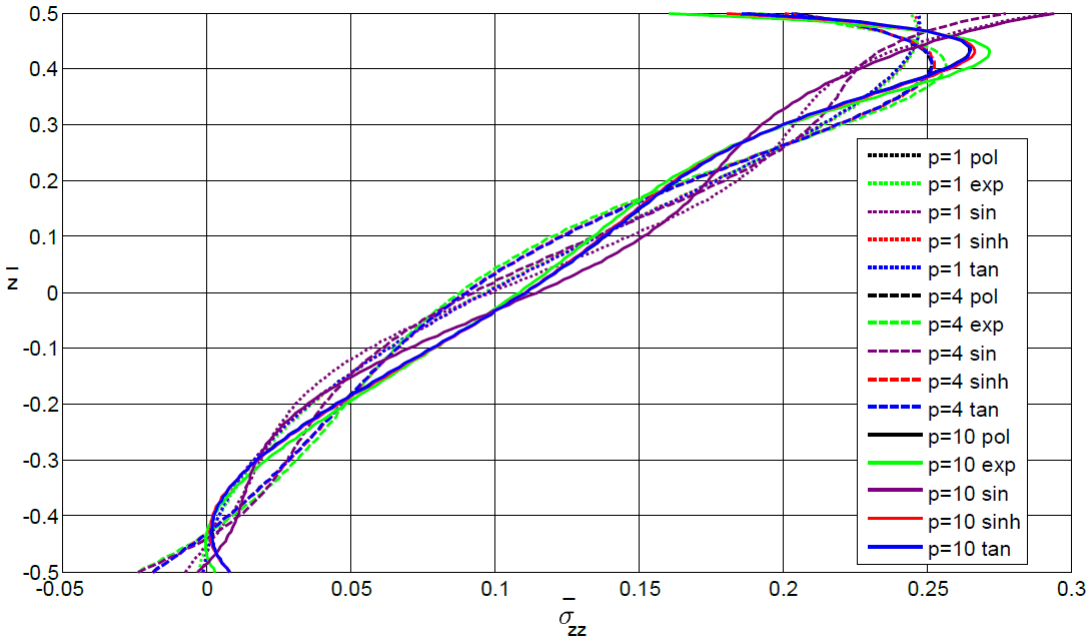

Figure 9.

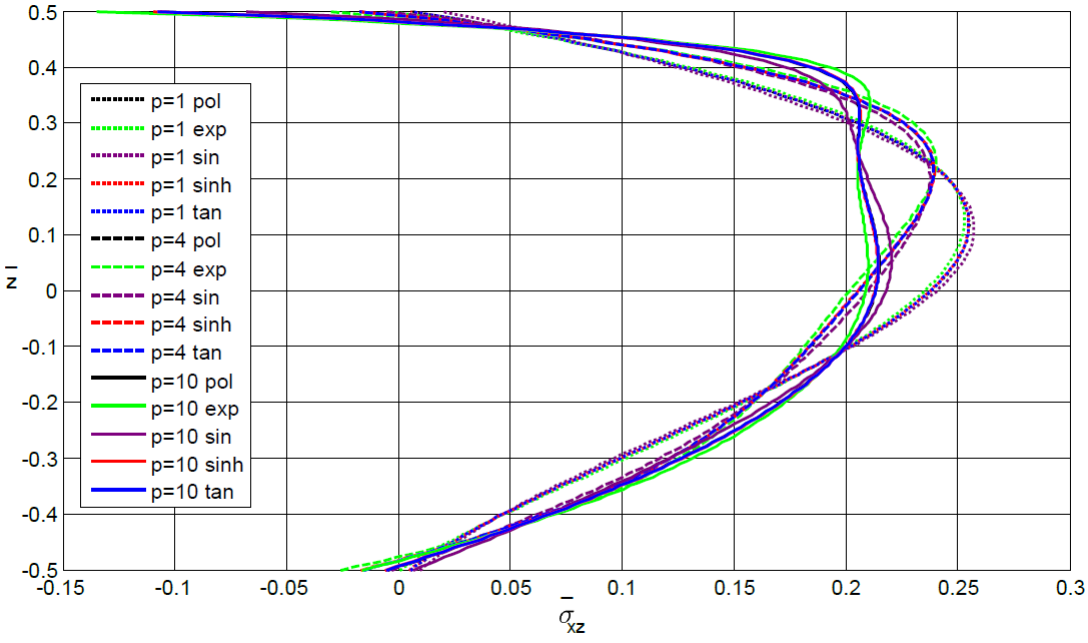

Figure 10.

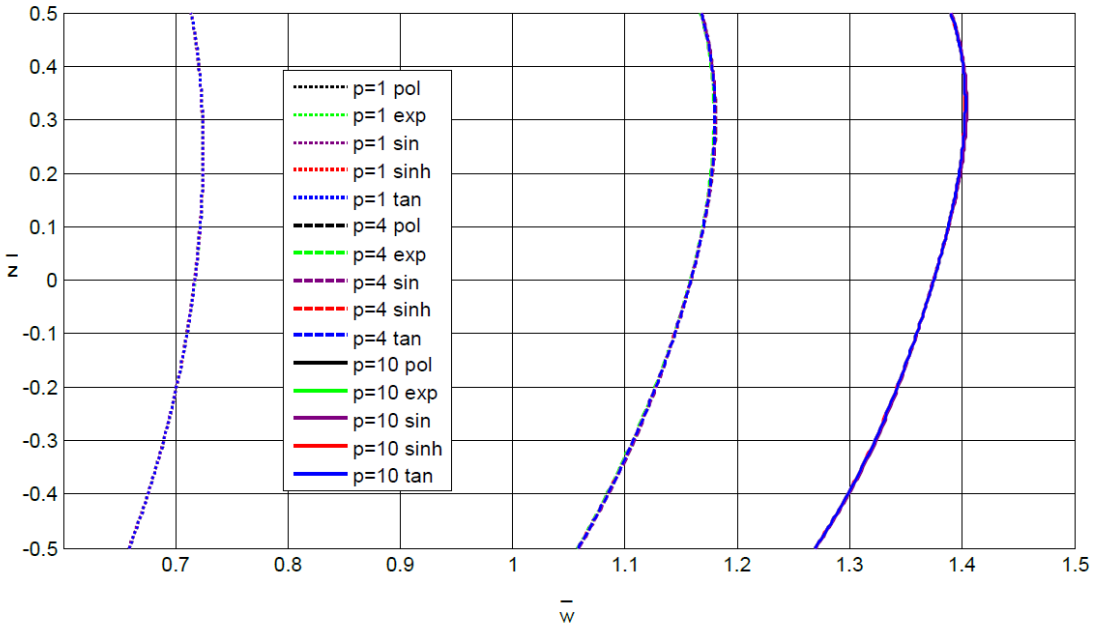

Figure 11.

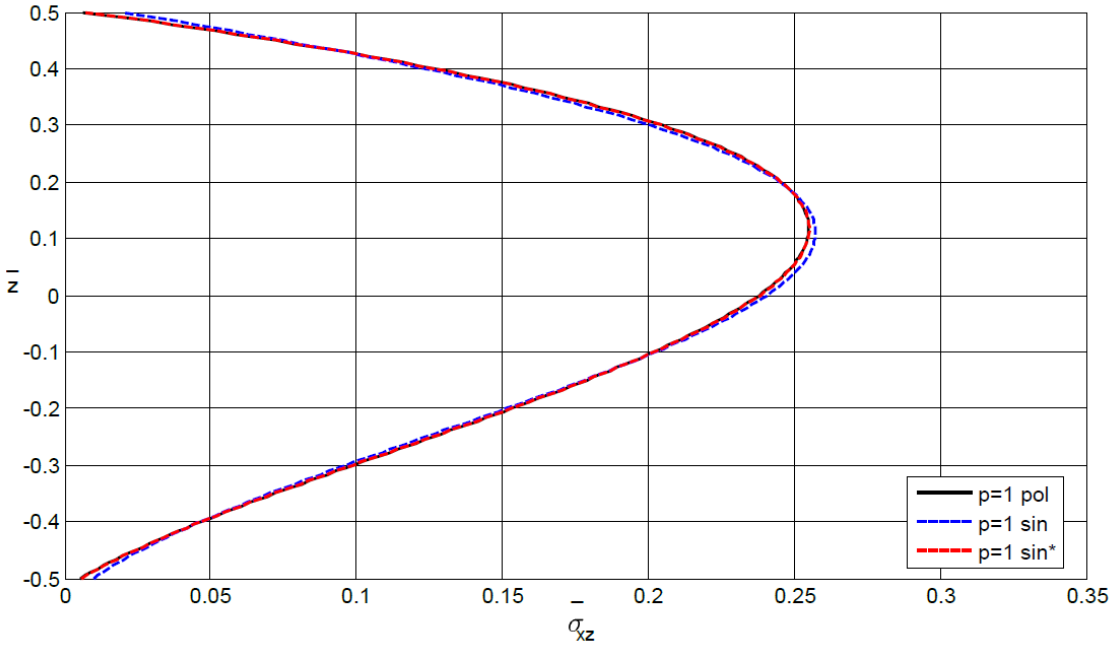

Figure 12.

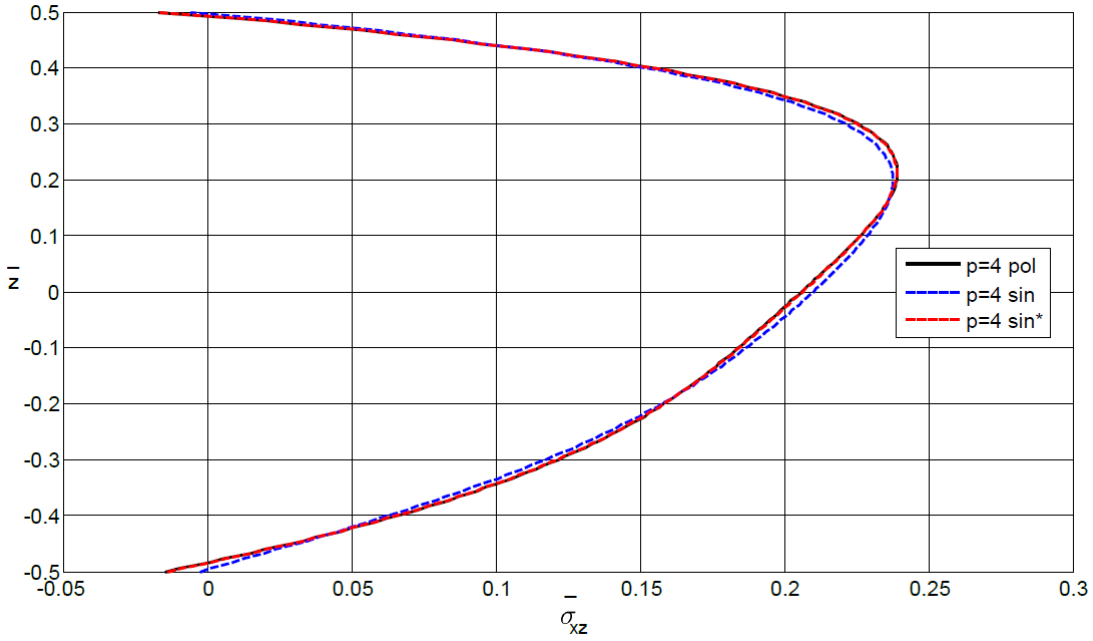

Figure 13.

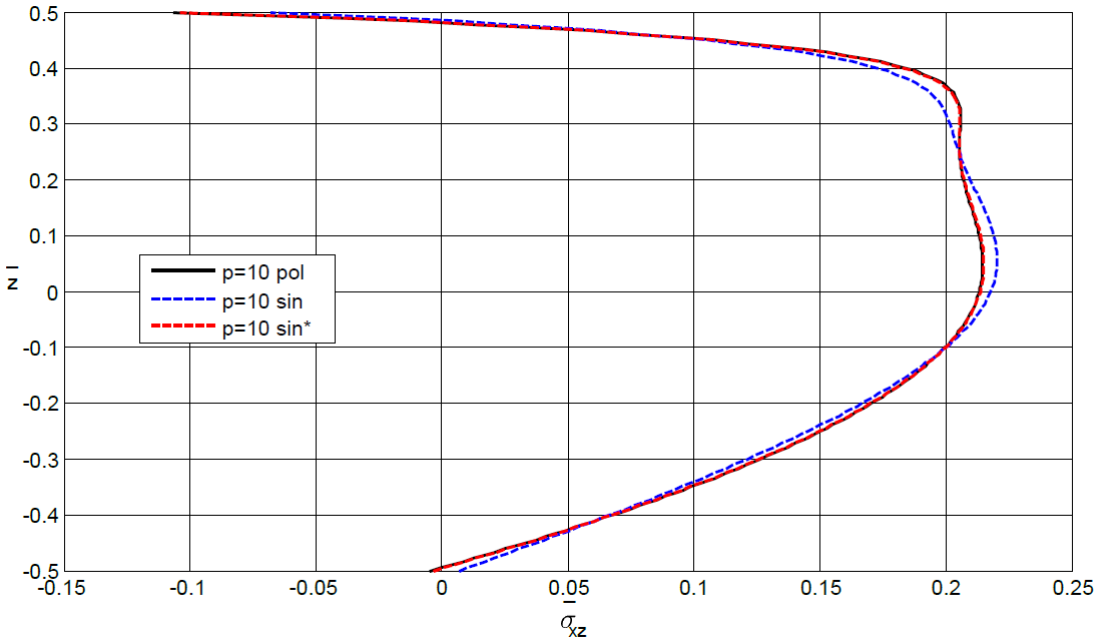

Figure 14.

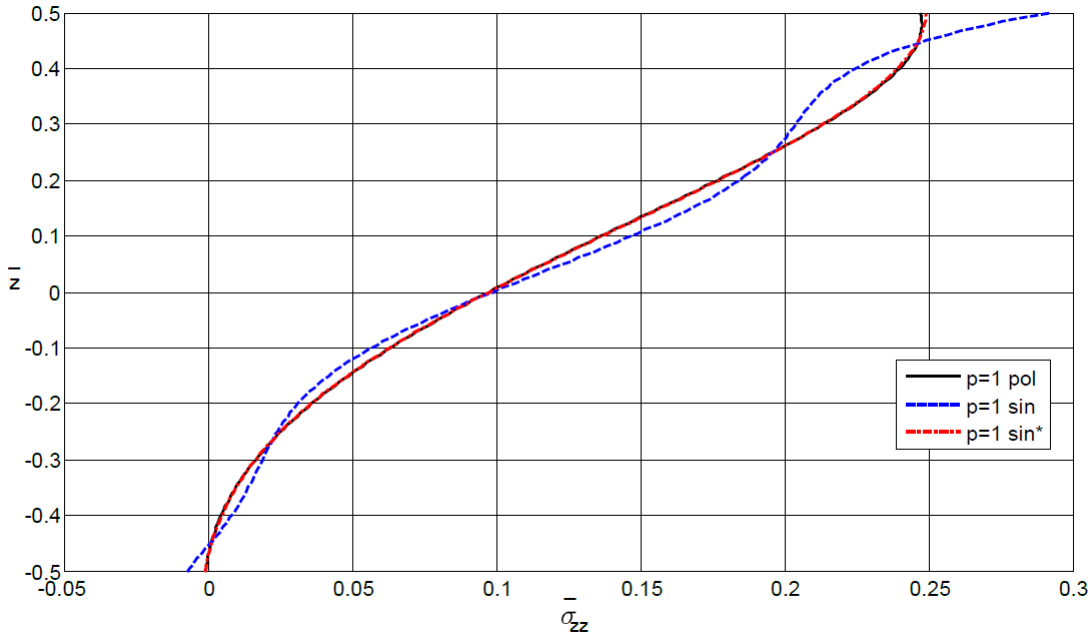

Figure 15.

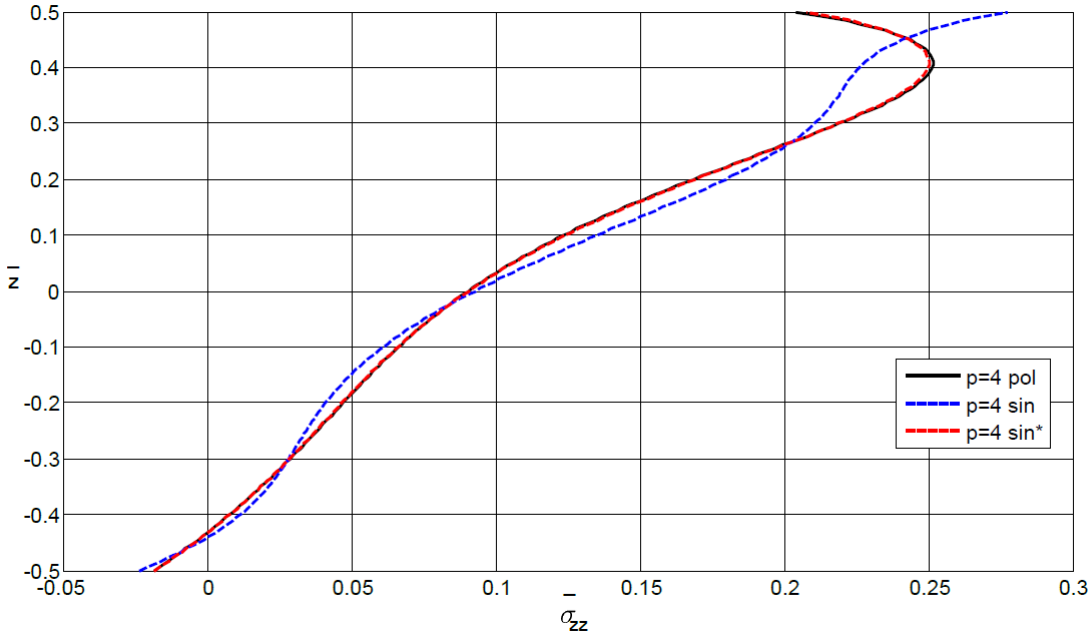

Figure 16.

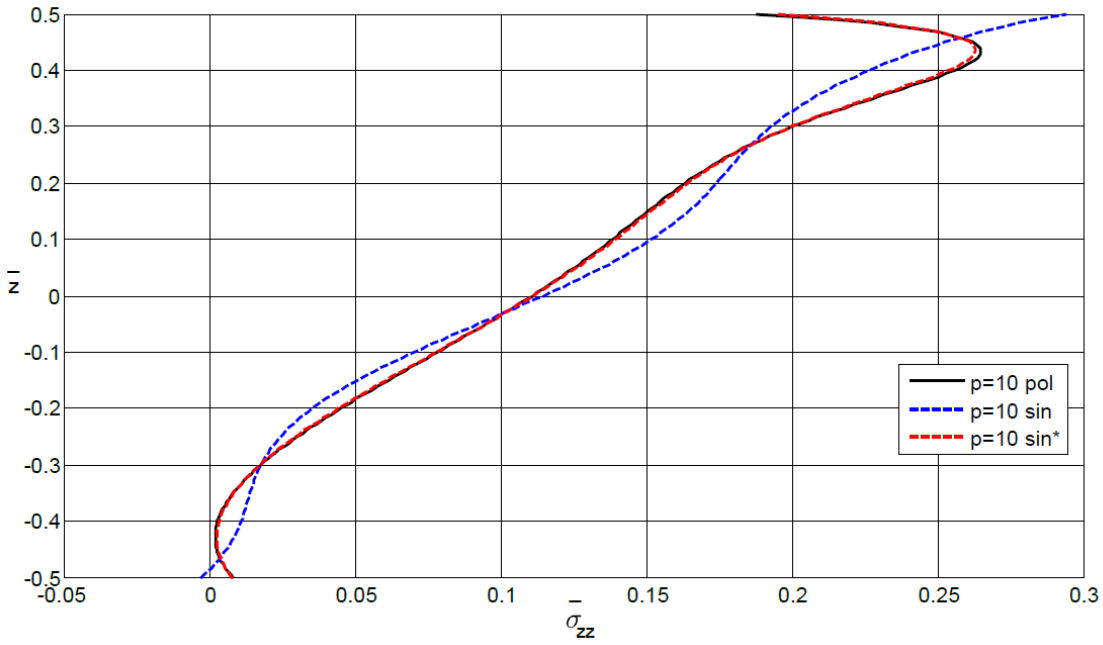

Figure 17.

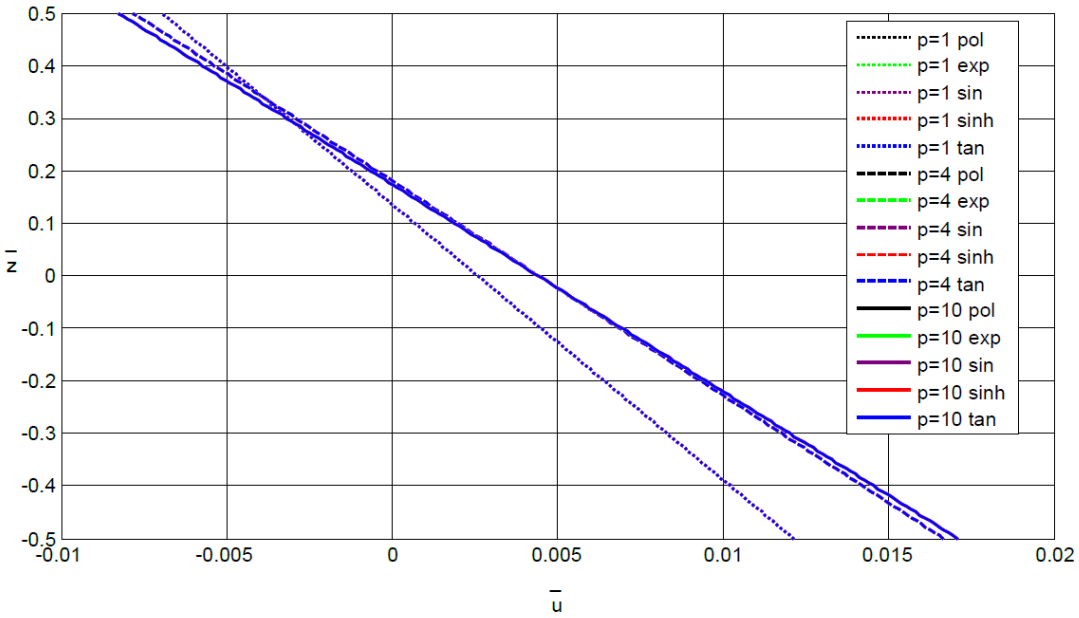

Figure 18.

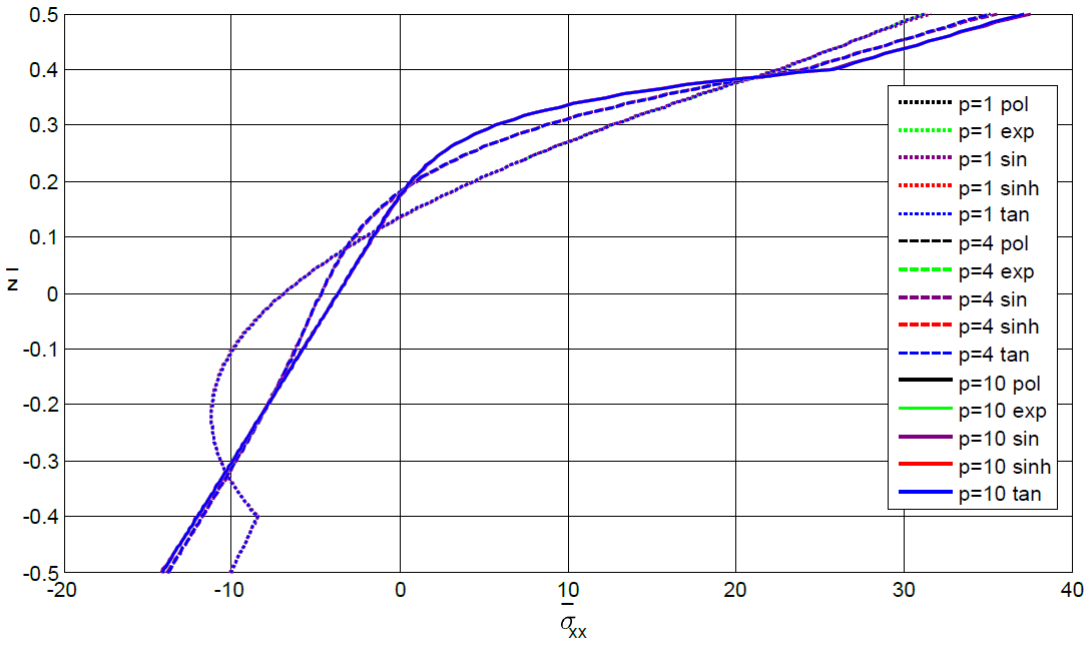

Figure 19.

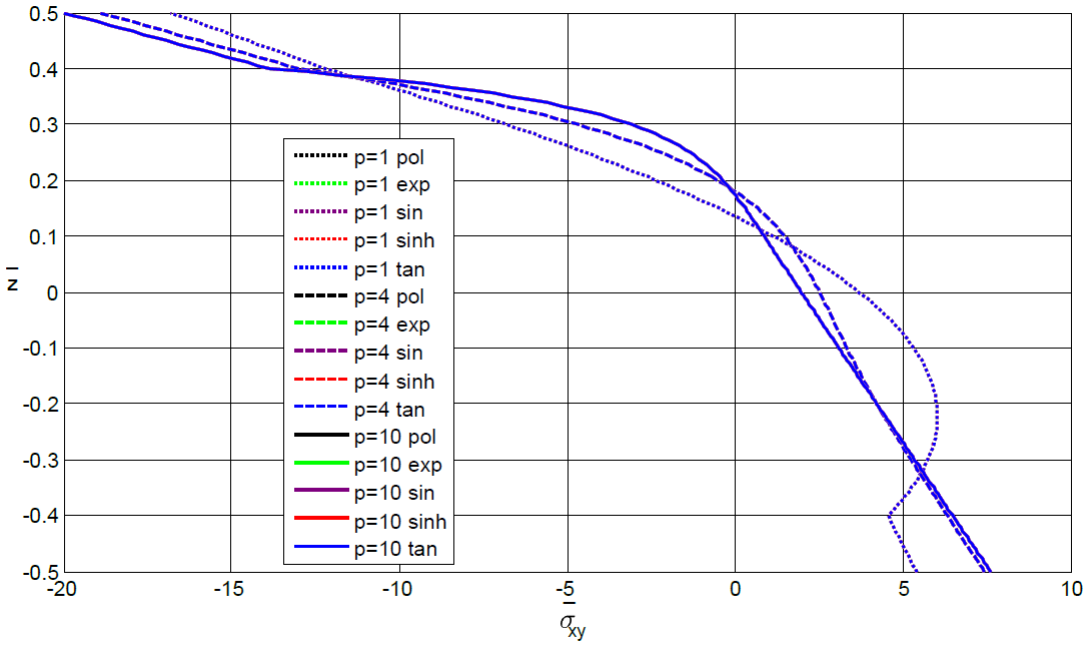

Figure 20.

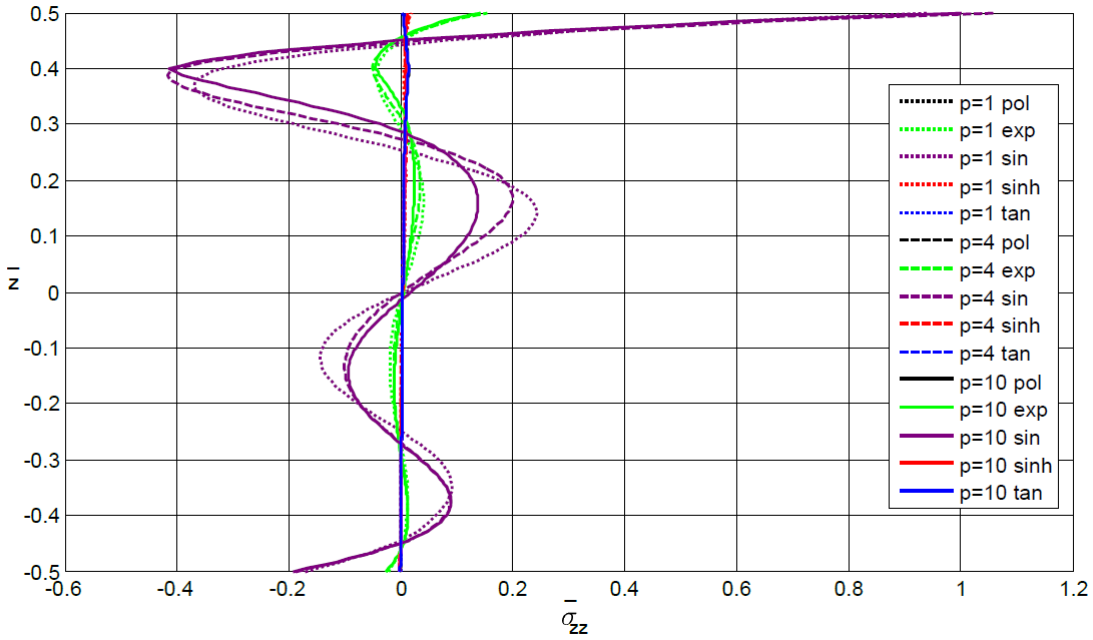

Figure 21.

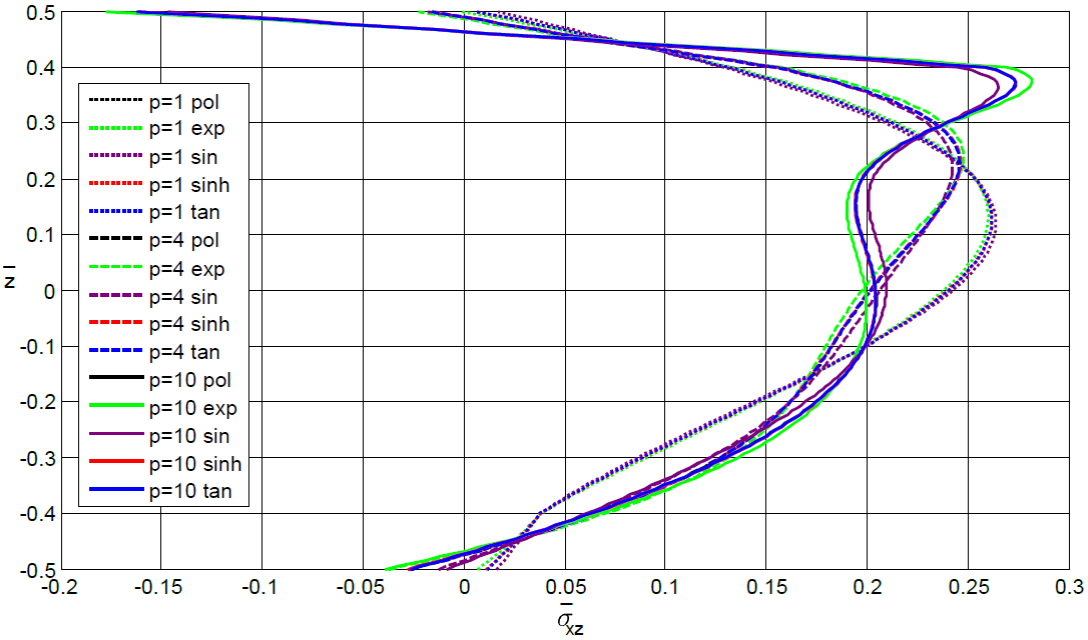

Figure 22.

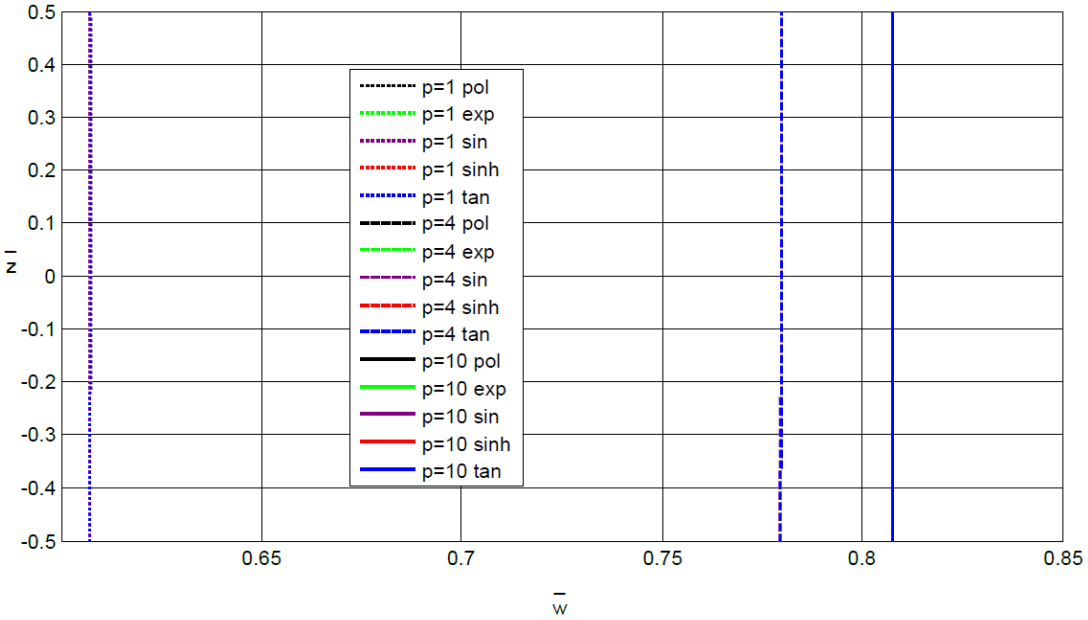

Figure 23.

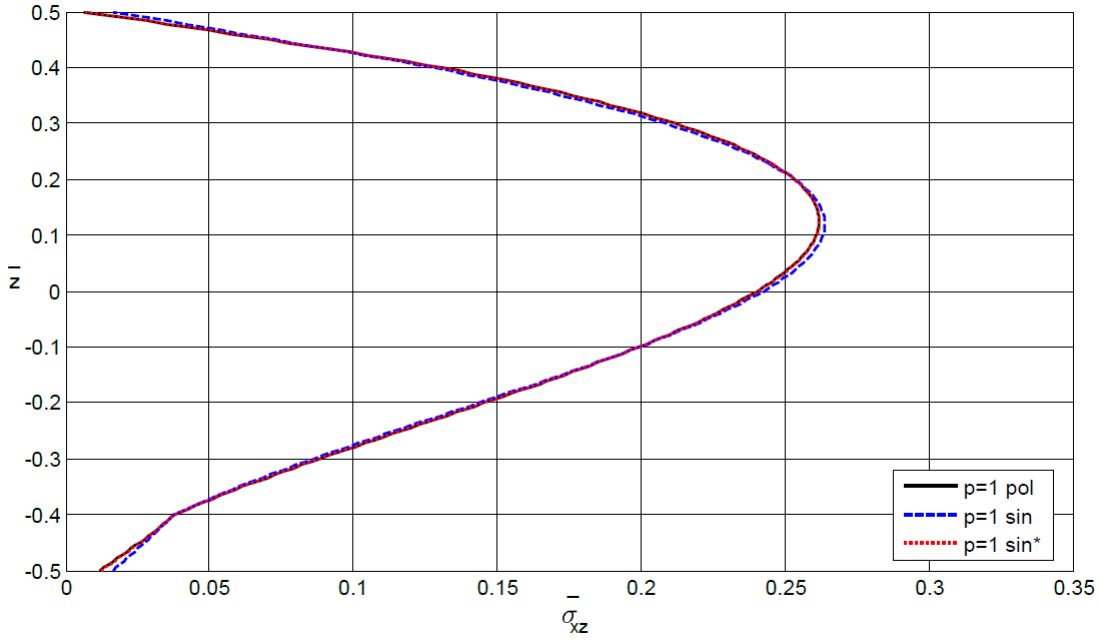

Figure 24.

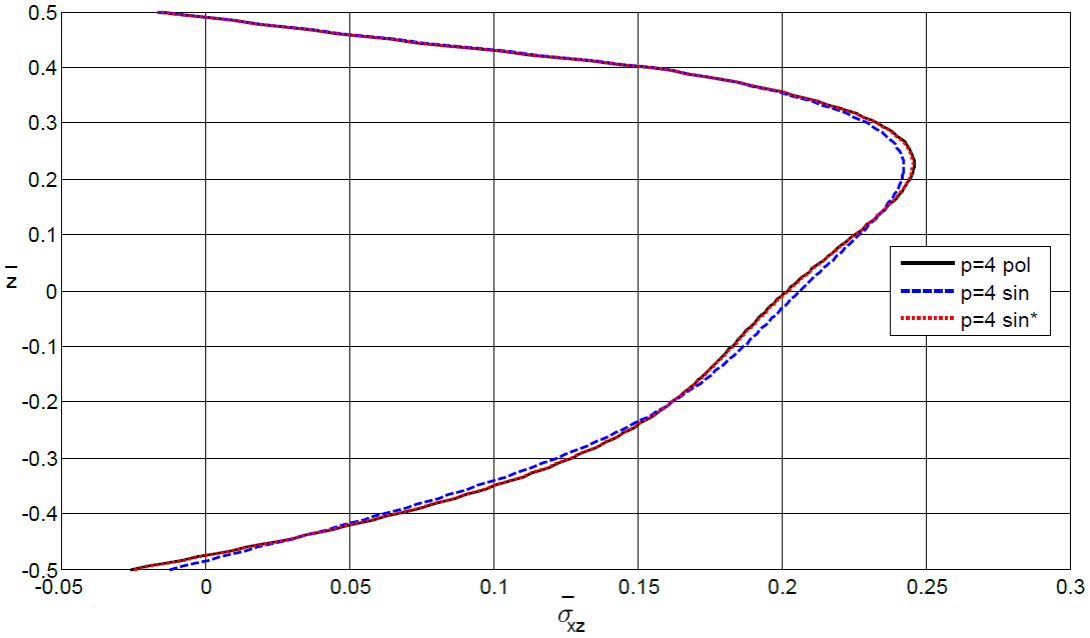

Figure 25.

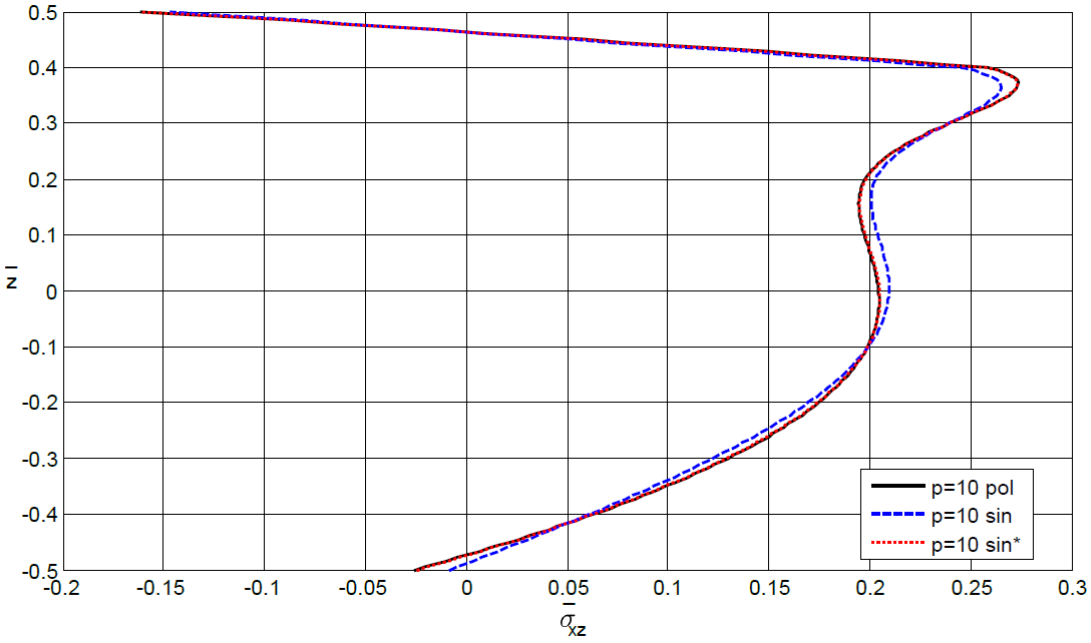

Figure 26.

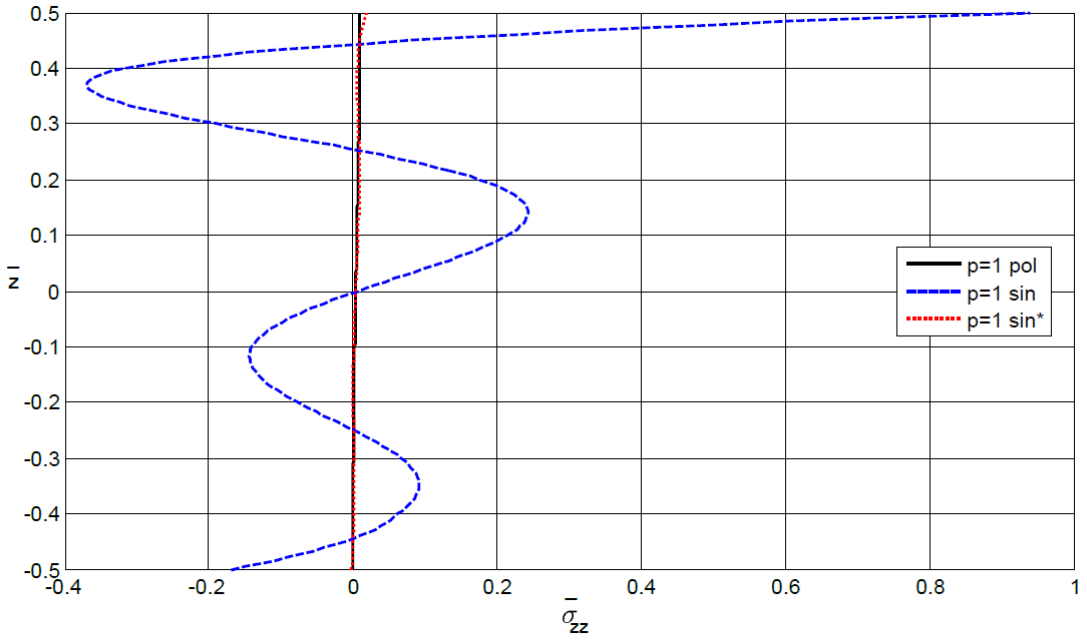

Figure 27.

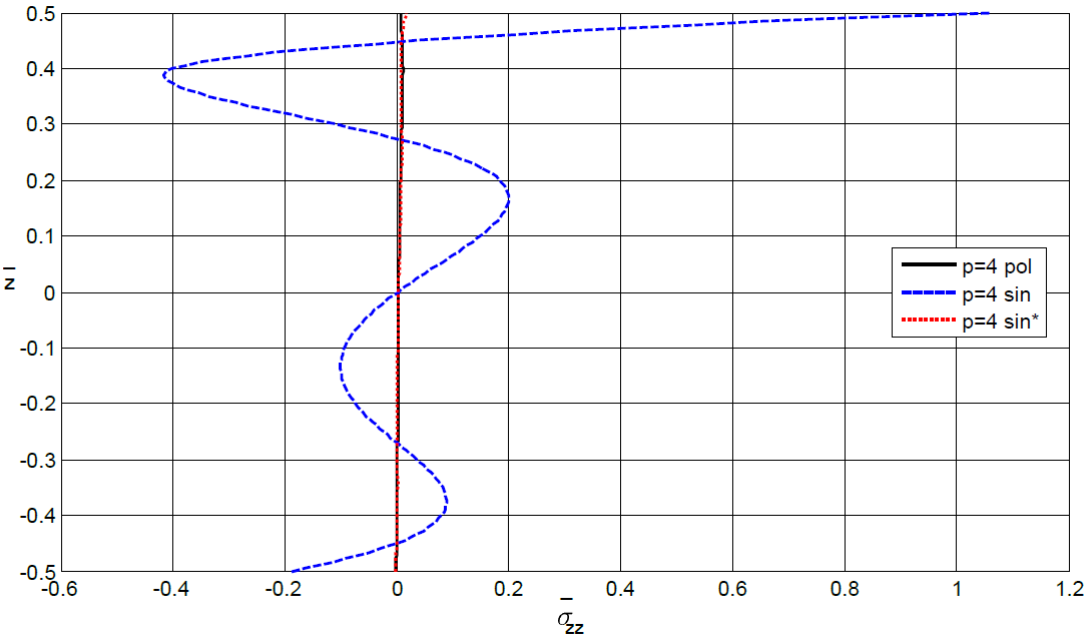

Figure 28.

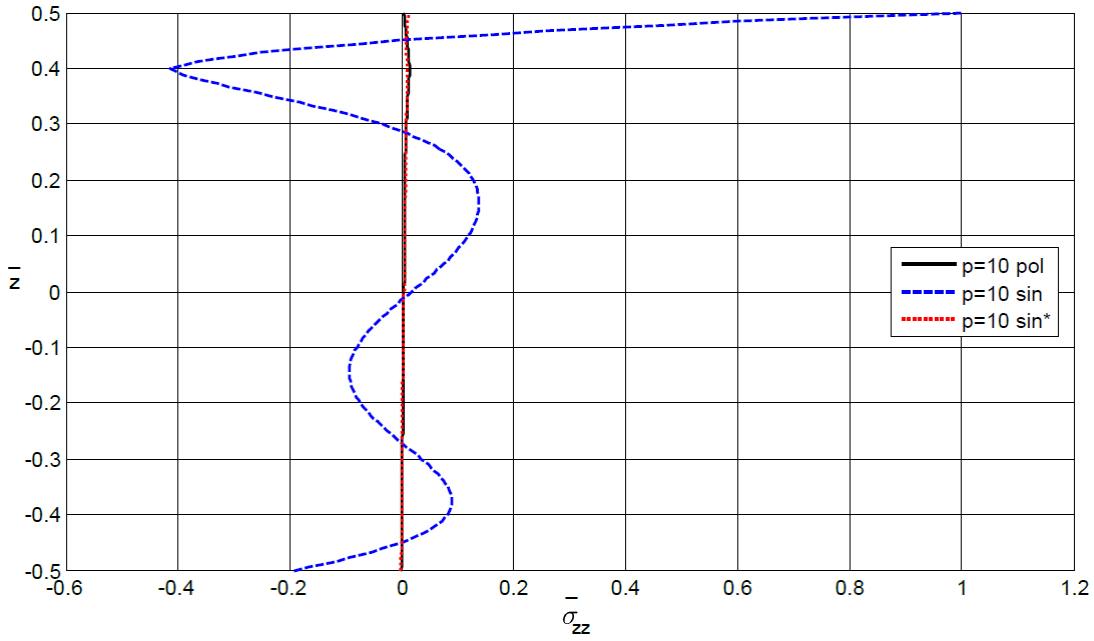
0.5
0.4
0.3
0.2
0.1
0
-0.1
-0.2
-0.3
-0.4
-0.5
z̄
-0.6
-0.4
-0.2
0
0.2
0.4
0.6
0.8
1
1.2
σ̄zz
p=10 pol
p=10 sin
p=10 sin*